
COMPOSE: Composing Future Theorems from Citations and Formal Structure

David Busbib Michael Werman

Hebrew University of Jerusalem

Abstract

A plausible future mathematical claim must satisfy two constraints: it should follow the direction of prior work and respect the formal dependencies that constrain what can validly follow. Existing approaches typically model only one of these sources, producing claims that are either weakly grounded or insufficiently motivated. We introduce grounded future mathematical generation, where the goal is to generate a plausible future theorem-like claim for an anchor paper using two complementary sources of context: its scientific citation graph and aligned formal theorem dependency graph. To address this setting, we propose COMPOSE, a dual-graph framework that conditions a language model on both scientific citation context and formal theorem structure. To support this setting, we construct a dataset of 108K paired scientific-formal graph examples from arXiv and Mathlib, together with a benchmark of 47K future papers from 2024–2025. Experiments show that COMPOSE outperforms strong baselines on retrieval to real future papers and achieves the best overall performance under LLM-judge evaluation, producing more grounded and mathematically richer outputs. These results show that future mathematical generation benefits from combining scientific context with formal structure. Project page is available at <https://david-busbib.github.io/COMPOSE-page/>.

1 Introduction

Large language models have shown growing promise in anticipating future scientific contributions from existing knowledge across many domains [Si et al., 2024, Lu et al., 2024a, Wang et al., 2026]. However, in the mathematical domain, a plausible future result must both extend the research trajectory of prior work [Lakatos, 1976, Davies et al., 2021] but also respect the logical dependencies that determine what can validly follow from existing definitions, lemmas, and theorems [Yang et al., 2023, Uskuplu et al., 2025, Cabral et al., 2025]. Thus, the task is not only to produce fluent mathematical text, but to generate a result that is both scientifically meaningful and logically grounded.

This challenge is reflected in two complementary sources of mathematical knowledge: scientific papers, which capture how ideas develop across the literature and indicate which directions are worth pursuing [Azher et al., 2025, Baek et al., 2025, He-Yueya et al., 2026], and formal theorem libraries such as Lean’s Mathlib, which encode mathematical results together with explicit dependency structure. Combining the two is non-trivial because the same content appears differently in each source, and because the two sources are organized by fundamentally different relational structures [Gao et al., 2024a, Zhang et al., 2025, Wu et al., 2022]. Yet existing approaches tackle only one side: models trained on scientific text alone can identify plausible research directions but may generate claims that are not grounded in formal mathematical dependencies [Wang et al., 2024b, Radensky et al., 2026, Baek et al., 2025, He-Yueya et al., 2026]; theorem-proving systems [Wang et al., 2025a, First et al., 2023, Yang et al., 2023] reason over formal structure but lack the surrounding scientific context needed to anticipate which directions are most promising; and structure-based methods

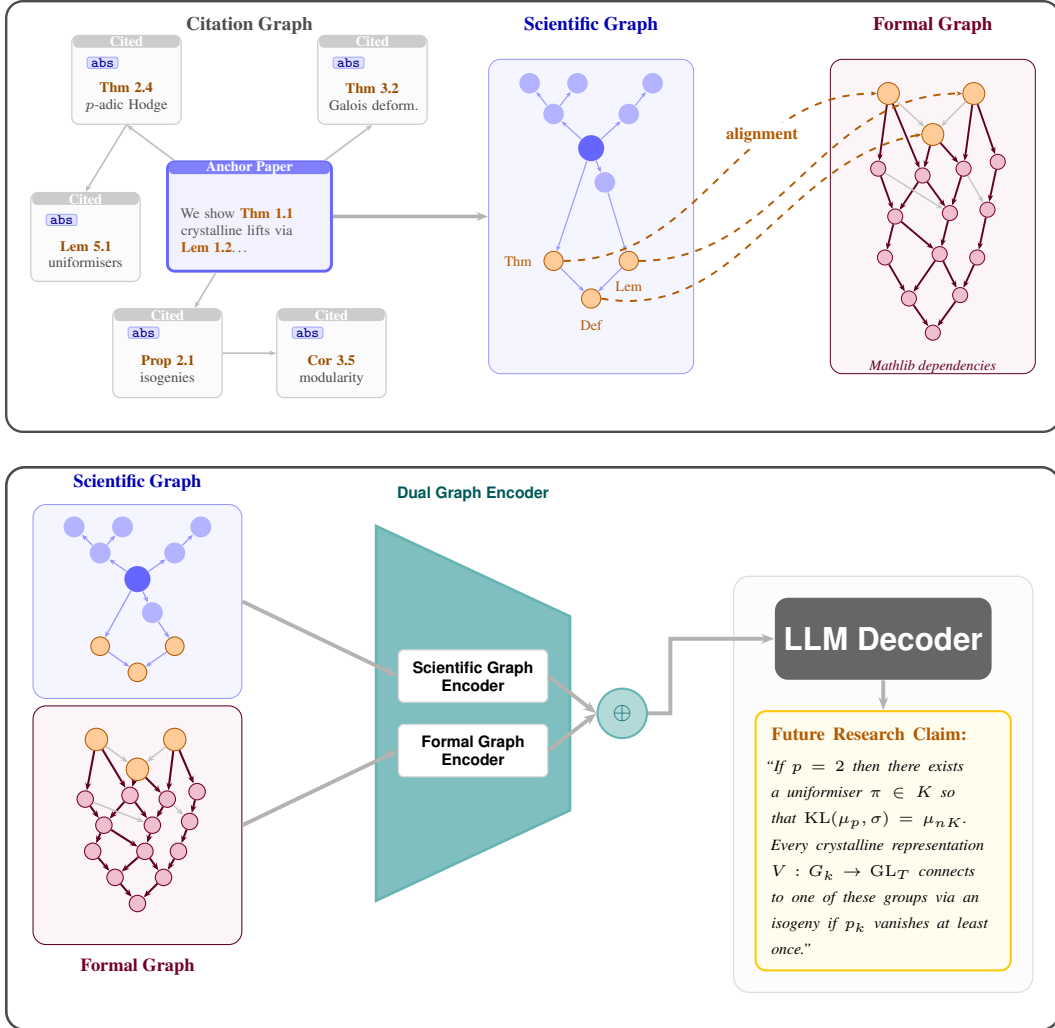


Figure 1: **Top: Data construction.** Given an anchor paper and its citation graph (left), we build its scientific graph (center) where **blue nodes** represent paper abstracts and **orange nodes** represent extracted theorems. Each informal theorem is matched to its corresponding Mathlib theorem (dashed arrows), and the matched theorems are then used in order to construct the paper’s formal graph of Lean dependencies (right). **Bottom: Model architecture.** The scientific graph and formal graph are encoded by dedicated GNNs, fused via cross-attention (\oplus), and used to condition a math-specialized LLM decoder that generates a *future research claim*.

typically model only one of these sources, using either citation structure [An et al., 2021] or theorem dependencies [Wang et al., 2025b, Zhu et al., 2026]. As a result, existing work still lacks a method that combines both sources for grounded future mathematical generation.

In this work, we propose *COMPOSE*, a system for generating plausible future mathematical claims from an anchor paper. This is carried out by jointly modeling scientific context and formal mathematical structure. To represent these two sources, we construct two complementary graphs: (i) a scientific graph built from the anchor paper, selected cited papers, and extracted theorems, and (ii) a formal graph built by aligning those theorems to corresponding formal theorems and their dependency structure. These two graphs are encoded separately and fused into a shared representation that conditions an LLM decoder on both the scientific direction of the papers and the formal structure of the underlying mathematics. Figure 1 provides an overview of the full pipeline. To learn this representation effectively, training proceeds in two stages: we first optimize the graph encoders and fusion module with alignment objectives, and then fine-tune the decoder for graph-conditioned generation. The model then generates a theorem-like mathematical text that represents a plausible

contribution in the same research direction, grounded in both the evolution of ideas across papers and the dependency structure of formal mathematics.

To evaluate this setting, we construct a benchmark of 108K paired samples from arXiv mathematics using training papers collected from the pre-2023 corpus, together with a test set of 47K papers from late 2024 and 2025.

Empirically, COMPOSE achieves the strongest retrieval performance in our main evaluation setting and performs best overall under LLM-judge evaluation, with ablations confirming that both graph sources contribute.

We make the following contributions:

- We study grounded future mathematical generation, where the goal is to predict plausible future mathematical claims using both scientific citation context and formal theorem dependencies.
- We construct a dataset of 108K paired scientific-formal graph samples from arXiv and Mathlib, using an informal-to-informal alignment strategy via FrenzyMath, and establish a benchmark of 47K future papers from 2024-2025 for evaluation.
- We propose COMPOSE, a system for grounded future mathematical generation that combines scientific citation context with formal theorem structure to generate plausible future mathematical claims.

2 Related Work

Future Scientific Generation. Prior work studies future scientific generation in several ways. One line of work generates future research directions from prior literature using retrieval or iterative retrieval-and-reasoning over related papers [Azher et al., 2025, Baek et al., 2025, Radensky et al., 2026]. Another line of work uses citation structure or temporal supervision for the task [Wang et al., 2026, 2024b]. GIANTS [He-Yueya et al., 2026] uses citation-based scientific context to guide generation, although it targets future scientific summaries rather than theorem-like claims. Some work also explores structure-aware scientific generation using external graphs or chain-of-ideas frameworks [Gao et al., 2025, Xiong et al., 2024]. Across these settings, existing systems rely on textual, citation-based, or structured scientific context, without combining the formal theorem structure that constrains what can validly follow from prior results.

Formal Mathematical Reasoning. Formal proof libraries such as Lean’s Mathlib [mathlib Community, 2020], Isabelle’s Archive of Formal Proofs [Paulson, 1994], and Coq-based libraries [Barras et al., 1999, Rudnicki, 1992] encode large collections of verified theorems together with their formal dependency structure [Li et al., 2024]. This dependency structure is not just a record of what has been proved; it also helps determine what can be proved next. Retrieval-augmented and premise-selection systems use this structure to identify relevant premises for proof search, as in ReProver [Yang et al., 2023] and related work [Alemi et al., 2017, Wang et al., 2017, Mikula et al., 2024]. Formal theorem provers also use this library context to guide proof generation and search, including systems such as Baldur [First et al., 2023] and DeepSeek-Prover [Xin et al., 2024], as well as more recent work [Wang et al., 2025a, Dong and Ma, 2025]. Beyond proof search, formal libraries have also been used to conjecture what should be proved in the first place: Lemmanaid [Alhessi et al., 2026] proposes new lemmas by drawing analogies across existing theories, while related work studies conjecture generation, verification, and blueprint construction from library context [Onda et al., 2025, Kasaura et al., 2025, Liu et al., 2026, Zhu et al., 2026]. Together, these systems show that formal dependency structure can inform not only how to prove but also what to prove. However, they operate entirely within the formal world, requiring formal input and producing formal output, without modeling the informal mathematical context found in research papers.

Scientific Informal-Formal Alignment. In our setting, the alignment problem is to match an informal theorem from a research paper to its corresponding theorem in Mathlib. A natural approach is to translate informal mathematics written in natural language into formal proof-assistant syntax. Early work used large language models to map informal theorems into formal representations Wu et al. [2022], Azerbayev et al. [2023], Lu et al. [2024b]. Later work improved Autoformalization with

stronger training, retrieval-based methods, and math-specialized models, including Kimina [Wang et al., 2025a], Draft, Sketch, and Prove [Jiang et al., 2023], and ProofBridge [Jana et al., 2026]. Despite these advances, coverage on real paper-level mathematics remains limited because of the large vocabulary gap between informal exposition and formal syntax Zhang et al. [2025]. As an alternative, FrenzyMath [Gao et al., 2024b] takes a different route by providing human-written informal descriptions for over 136K Mathlib theorems, enabling informal-to-informal retrieval as a pragmatic alignment strategy that avoids formalization altogether. Recent work also suggests that linking informal theorem to formal libraries benefits from stronger retrieval and intermediate structure [Lu et al., 2024b, Jiang et al., 2023, Jana et al., 2026]. Unlike these works, we do not treat informal-formal alignment as the primary objective. Instead, we use the resulting aligned structure to support grounded generation of future mathematical claims.

3 Method

Given an anchor paper, the goal is to generate a plausible future mathematical claim using its scientific and matched formal context. Our approach has three components. First, we construct a dataset that links scientific papers with formal theorem graphs 3.1. Second, we introduce COMPOSE, a dual-encoder architecture that jointly models scientific and formal mathematical structure 3.2. Third, we present our two-stage training 3.3.

Inference overview. At inference time, given an anchor paper, the model constructs two graphs: a scientific citation graph G_s , built from the paper and its contextually relevant cited papers, and a formal theorem dependency graph G_f , built from Mathlib theorems aligned to extracted mathematical theorems. Each graph is independently encoded by a dedicated GNN encoder. The two representations are then fused via cross-attention. The fused graph embeddings are passed as conditioning to our language model decoder, which generates a free-text theorem proposal.

3.1 Data Curation and Construction

Training our dual-graph model requires paired examples linking scientific context with formal theorem-dependency structure. We construct this dataset by linking mathematical papers collected via S2ORC [Lo et al., 2020] with formal theorems from Mathlib [mathlib Community, 2020].

On the scientific side, we begin with an anchor paper and construct outgoing citation edges for up to two hops, retaining at most 5 cited papers at the first hop and at most 3 cited papers per node for the second hop. Cited papers are selected by citation-context relevance, favoring citations that are discussed in important parts of the paper or used directly in its proofs or main results, rather than by including the full citation list; full selection details are in Appendix A.1. The graph contains *abstract* nodes for all included papers, together with *theorem* nodes extracted from papers in the first two citation hops. Each *theorem* node is connected either to its corresponding *abstract* node or to a parent *theorem* node. We use typed edges to distinguish citation links, paper-to-theorem links, and theorem-to-theorem links, allowing the graph to capture both external and internal citation context. For each example, we also identify a target paper: a paper that cites the anchor and was published after it, excluded from the input graph. Its main mathematical claim serves as the generation target.

On the formal side, we align extracted theorems to Mathlib theorems using dense retrieval over the FrenzyMath corpus [Gao et al., 2024b], which provides informal descriptions for 140k Mathlib theorems (see Figure 2). For each extracted theorem, we keep the top retrieved theorem only if its similarity is above a threshold τ ; weak matches are discarded. Each retained theorem serves as the root of the local formal dependency graph, which is expanded for a fixed number of hops using directed theorem-dependency edges extracted from Mathlib with LeanDojo [Yang et al., 2023]. Root nodes are marked with a distinct node type, while the remaining nodes represent dependency neighbors. A comparison with alternative alignment strategies and additional details about τ is provided in Appendix A.4.

Starting from a corpus of 500K mathematical papers published between 2000 and 2023, this process yields approximately 108K paired paper-theorem subgraphs. In

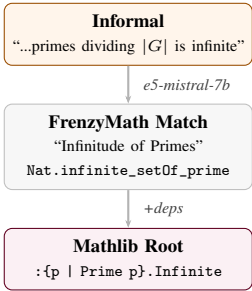


Figure 2: Informal-to-informal alignment.

addition, we define a temporally held-out benchmark of 47K mathematical papers from late 2024 and 2025, using their *abstract* and extracted main claim, as future target texts for evaluation. Full details of the alignment procedure, target construction, filtering steps, and dataset statistics are provided in Appendix A.

3.2 COMPOSE

We first introduce notation, then present the encoder, fusion, and decoder components.

Formally, each example is represented as

$$x = (G_s, G_f, \mathcal{P}), \quad G_s = (V_s, E_s), \quad G_f = (V_f, E_f),$$

where x is the input context and $y = (y_1, \dots, y_T)$ is the target output sequence.

The scientific graph contains two types of nodes:

$$V_s = \{v_j^{\text{abs}}\}_{j=1}^n \cup \{u_i^{\text{thm}}\}_{i=1}^m,$$

where v_j^{abs} denotes an abstract node corresponding to a paper in the scientific graph, and u_i^{thm} are extracted theorem nodes. The edge set E_s contains directed citation edges between abstract nodes and structural edges connecting each theorem node either to its corresponding abstract node or to a parent theorem node.

The formal graph contains theorem nodes, $V_f = \{v_\ell^{\text{thm}}\}_{\ell=1}^k$, where each node corresponds to a Mathlib theorem, and edge set E_f is given by dependency relations extracted from Mathlib.

Let $V_s^{\text{thm}} = \{u_i^{\text{thm}}\}_{i=1}^m$ denote the set of theorem nodes in G_s . The alignment set is defined as

$$\mathcal{P} \subseteq V_s^{\text{thm}} \times V_f,$$

where each pair $(u^{\text{thm}}, v^{\text{thm}}) \in \mathcal{P}$ links an informal theorem node in G_s to its matched formal theorem node in G_f .

Each graph is processed by a dedicated GNN encoder. The two encoders share the same overall message-passing architecture Gilmer et al. [2017] but differ in their node type and input initialization. In G_s , nodes are heterogeneous, with abstract and theorem nodes initialized from E5 embeddings [Wang et al., 2024a]. In G_f , nodes correspond to formal Lean theorems and are initialized from DeepSeek-Math embeddings [Shao et al., 2024] of theorem signatures, chosen for their stronger representation of formal mathematical content. Both encoders use directed, edge-type-specific message passing, with incoming and outgoing messages aggregated separately. The resulting updates are combined with a learned gated residual connection to mitigate over-smoothing, followed by layer normalization. For each node, the GNN produces a structural vector that is concatenated with the node’s original text embedding, yielding contextualized representations \mathbf{h}_i^s and \mathbf{h}_j^f that capture both semantic content and graph structure. Full architectural details are in Appendix B.

Since G_s and G_f operate in different representation spaces, we project \mathbf{h}_i^s and \mathbf{h}_j^f into a shared latent space using the same learned MLP. Type embeddings are then added after projection to distinguish nodes from G_s and G_f . We apply a single bidirectional cross-attention block between the two node sets, with separate Q/K/V projections for the scientific-to-formal and formal-to-scientific directions, and residual connections with layer normalization applied after each directional update. The resulting fused node representations are denoted by $\{\tilde{\mathbf{h}}_i\}_{i=1}^{|V_s|+|V_f|}$.

The fused node representations $\{\tilde{\mathbf{h}}_i\}$ are provided as graph inputs to a pretrained math-specialized language model decoder adapted with LoRA Hu et al. [2021]. Cross-attention layers are inserted at regular intervals, covering approximately 20% of the decoder layers. In these layers, the decoder hidden states serve as queries, while the fused graph node representations, projected to the decoder hidden dimension, serve as keys and values. This allows each generation step to attend over the full set of fused graph nodes, conditioning the output sequence y on both the scientific context of G_s and the formal structure of G_f .

3.3 Two-Stage Training

We train the model in two stages. The first learns graph representations that capture both within-graph structure and alignment between the scientific and formal domains, without using the decoder.

The second adds the decoder and fine-tunes the full model for generation while preserving graph conditioning.

In the first stage, we train the scientific and formal graph encoders, together with the bridge MLP and fusion module, while keeping the pretrained text embeddings frozen. The resulting graph modules are then used to initialize the second stage. The first-stage objective is:

$$\mathcal{L}_{\text{stage}_1} = \lambda_{\text{link}} \mathcal{L}_{\text{link}} + \lambda_{\text{align}} \mathcal{L}_{\text{align}} + \lambda_{\text{cross}} \mathcal{L}_{\text{cross}} \quad (1)$$

To ensure both encoders capture graph structure rather than collapsing to uniform representations, we supervise them with a link prediction loss. For each graph $G \in \{G_s, G_f\}$, we define $a_{ij} = 1$ if $(v_i, v_j) \in E$ and $a_{ij} = 0$ for non-edges, and optimize

$$\mathcal{L}_{\text{link}} = -\mathbb{E} [a_{ij} \log \sigma(\mathbf{h}_i \cdot \mathbf{h}_j) + (1 - a_{ij}) \log (1 - \sigma(\mathbf{h}_i \cdot \mathbf{h}_j))] . \quad (2)$$

where \mathbf{h}_i and \mathbf{h}_j denote representations in the graph under consideration, and σ is the sigmoid function.

To encourage the fused graph representation to align with the scientific and formal content of the target, we use a contrastive alignment loss [van den Oord et al., 2019]. Let

$$\tilde{\mathbf{h}}_G = \text{AttnPool}(\{\tilde{\mathbf{h}}_i\}_{i=1}^{|V_s|+|V_f|}) \quad (3)$$

denote the fused graph representation obtained by attention pooling over the fused node representations.

We construct a positive target representation \mathbf{e}^+ from the held-out target paper by combining the embeddings of its abstract and main mathematical claim, after projecting both into the shared latent space. For each example, we construct negative target representations \mathcal{B}^- from papers that don't cite papers in the current scientific subgraph, together with their main mathematical claim.

This objective encourages the fused graph representation to be close to the true held-out target and far from unrelated target papers. We then optimize

$$\mathcal{L}_{\text{align}} = -\log \frac{\exp(\text{sim}(\tilde{\mathbf{h}}_G, \mathbf{e}^+)/\tau)}{\exp(\text{sim}(\tilde{\mathbf{h}}_G, \mathbf{e}^+)/\tau) + \sum_{\mathbf{e}^- \in \mathcal{B}^-} \exp(\text{sim}(\tilde{\mathbf{h}}_G, \mathbf{e}^-)/\tau)} \quad (4)$$

where $\text{sim}(\cdot, \cdot)$ denotes cosine similarity.

Finally, to bridge the informal and formal spaces, $\mathcal{L}_{\text{cross}}$ aligns each informal theorem node $u_i^{\text{thm}} \in V_s$ with its matched theorem node $v_j^{\text{thm}} \in V_f$, where $(u_i^{\text{thm}}, v_j^{\text{thm}}) \in \mathcal{P}$. For each positive pair, we sample a set of random negative theorem nodes $\mathcal{N}_i \subset V_f$. We then optimize

$$\mathcal{L}_{\text{cross}} = -\frac{1}{|\mathcal{P}|} \sum_{(u_i^{\text{thm}}, v_j^{\text{thm}}) \in \mathcal{P}} \log \frac{\exp(\hat{\mathbf{h}}_i^s \cdot \hat{\mathbf{h}}_j^f / \tau)}{\exp(\hat{\mathbf{h}}_i^s \cdot \hat{\mathbf{h}}_j^f / \tau) + \sum_{v_l^{\text{thm}} \in \mathcal{N}_i} \exp(\hat{\mathbf{h}}_i^s \cdot \hat{\mathbf{h}}_l^f / \tau)} . \quad (5)$$

where τ is the temperature hyperparameter.

In the second stage, we add a pretrained math-specialized decoder adapted via LoRA [Hu et al., 2021] and fine-tune the full model for graph-conditioned generation using two objectives: an autoregressive generation loss and a graph margin loss that prevents the decoder from ignoring the graph context. The autoregressive loss is:

$$\mathcal{L}_{CE} = -\sum_{t=1}^T \log p(y_t | y_{<t}, G_s, G_f) . \quad (6)$$

To prevent the decoder from ignoring the graph context and relying purely on language patterns, we additionally use a graph margin loss $\mathcal{L}_{\text{margin}}$ that requires the model to assign lower generation loss to the correct graph pair (G_s, G_f) than to a mismatched pair (G'_s, G'_f) sampled from a different citation graph within the same mathematical domain.

$$\mathcal{L}_{\text{margin}} = \max(0, \mathcal{L}_{CE}(G_s, G_f) - \mathcal{L}_{CE}(G'_s, G'_f) + \delta) \quad (7)$$

The second stage objective is

$$\mathcal{L}_{\text{stage}_2} = \lambda_{ce} \mathcal{L}_{CE} + \lambda_{\text{margin}} \mathcal{L}_{\text{margin}} \tag{8}$$

Additional alignment and training details are provided in Appendix B.

4 Experiments

4.1 Experimental Setup

Data and Temporal Split. The 108K paired scientific-formal graph samples are split 80/10/10 into training, validation, and test sets. To evaluate temporal generalization, we construct a future-paper benchmark from a corpus of 47K mathematics papers published in late 2024-2025. We retain only test-set anchor papers that are cited by at least one paper in the 47K future-paper pool, yielding 2K test samples. For each anchor, future papers that cite it are treated as targets.

Retrieval Evaluation. Existing mathematical embedding models cluster future papers so tightly that the similarity gap between true target papers and randomly sampled unrelated papers is too small to reliably distinguish generation methods (see Appendix D.1). We therefore fine-tune a DeepSeek-Math embedding model on the 47K benchmark papers using a margin-ranking objective that pulls together papers with overlapping citation context and pushes apart unrelated papers. The resulting fixed model is then used as a shared retrieval evaluator for all compared methods.

Metrics. We report Tgt-Sim, the mean cosine similarity between the generated text and its corresponding ground-truth future papers; Neg-Sim, the mean cosine similarity between the generated text and 500 sampled papers from unrelated subfields of the future pool; Gap = Tgt-Sim – Neg-Sim, which measures how much closer the generated text is to the correct future papers than to unrelated ones in the pool; and H@k, the fraction of examples for which a relevant future paper appears in the top-k retrieved results. Exp-Sim measures similarity to the broader cluster of future papers that share citation context with the target, capturing whether the generated text lands in the correct research neighborhood rather than an unrelated area. We also report Novel Mathematical Claim Prediction (NMCP) metrics for theorem-level grounding: Precision, the fraction of outputs aligned with the formal theorem target derived from the future paper; Match, the fraction of outputs aligned with the natural-language theorem target from the future paper; and Math, the ratio of mathematical tokens in the output. To complement embedding-based metrics, we also evaluate generation quality using an LLM judge (see Section D).

Internal Variants. We compare **COMPOSE** against several internal variants that remove or simplify parts of the proposed system: (1) Paper-graph-only, which uses only the scientific graph G_s ; (2) Bag-of-Papers, which replaces the citation graph with a set of abstract and theorem nodes, removing graph structure and bypasses the two graph encoders; (3) Text-only (LoRA), which fine-tunes the decoder on our dataset using only a textual prompt, without any graph input; and (4) Prompt-only, which uses a richer prompt but does not use graph input or fine-tuning.

We evaluate all variants with both DeepSeek-Math 7B and Mistral 7B decoders to demonstrate that the gains from dual-graph conditioning are consistent across different backbone architectures.

Baselines. Since no prior work addresses exactly the same task, we compare against the closest systems for future scientific generation and future-paper prediction. These include (1) GIANTS [He-Yueya et al., 2026], which uses its own Qwen-based decoder; (2) DeepSeek-Math-7B-based systems, including FutureGen [Azher et al., 2025], GoAI [Gao et al., 2025], and KG-CoI [Xiong et al., 2024], which use the raw DeepSeek-Math-7B decoder; and (3) GPT-4.0-based variants of GoAI, CoI, and ResearchAgent [Baek et al., 2025], which we include as API baselines. We also include a simple retrieval baseline: Fixed NN, which retrieves by nearest-neighbor similarity over abstracts and main theorems. For all external baselines, we use the authors’ released code and follow the prompts described in their papers, adapting only the output request toward a mathematical claim.

4.2 Main Results

Table 1 compares internal model variants on the full test set. **COMPOSE** achieves the best results across all retrieval metrics, with the largest Gap (0.240), showing that its outputs stay closer to the

Table 1: Main results. *Retrieval* columns measure whether the generated theorem retrieves the correct future paper (47K pool). *NMCP* measures novel mathematical concept prediction against future theorems. Generation quality metrics are reported in Appendix C.

Decoder	Model	Future Retrieval (<i>thm-ft pool</i>)					NMCP		
		Tgt-Sim	Neg-Sim	Gap	H@10	H@100	Prec.	Match	Math
DeepSeek-Math 7B	Paper-graph-only	0.438	0.274	0.164	0.390	0.695	0.504	0.713	0.061
	Bag-of-Papers	0.399	0.271	0.128	0.230	0.544	0.497	0.719	0.064
	Text-only (LoRA)	0.463	0.287	0.176	0.369	0.738	0.302	0.356	0.076
	Prompt-only	0.471	0.297	0.174	0.109	0.345	0.165	0.187	0.051
	COMPOSE (ours)	0.525	0.285	0.240	0.508	0.808	0.560	0.730	0.083
Mistral 7B	Paper-graph-only	0.315	0.278	0.037	0.142	0.484	0.266	0.266	0.040
	Bag-of-Papers	0.418	0.279	0.139	0.154	0.506	0.323	0.211	0.070
	Text-only (LoRA)	0.443	0.291	0.152	0.091	0.359	0.425	0.450	0.068
	Prompt-only	0.447	0.296	0.151	0.090	0.197	0.575	0.653	0.044
	COMPOSE (ours)	0.451	0.290	0.161	0.348	0.697	0.554	0.671	0.054

Table 2: Future paper retrieval on the 2K test set (47K pool), comparing COMPOSE against baselines including open-source and API-based models.

Decoder	Model	Tgt-Sim	Neg-Sim	Gap	Exp-Sim	H@10	H@100
Retrieval	Fixed NN (abstracts+ main theorem)	0.393	0.285	0.108	–	0.068	0.392
DeepSeek-Math 7B	GoAI	0.510	0.309	0.202	0.381	0.376	0.680
	Prompt-only	0.487	0.276	0.211	0.352	0.348	0.697
	FutureGen	0.451	0.289	0.162	0.347	0.136	0.388
	CoI	0.469	0.311	0.158	0.377	0.340	0.640
GPT-4.0	GoAI-GPT	0.454	0.306	0.148	0.336	0.200	0.565
	CoI-GPT	0.486	0.310	0.176	0.336	0.410	0.770
	ResearchAgent-GPT	0.457	0.304	0.152	0.336	0.230	0.520
GIANTS	GIANTS	0.489	0.282	0.207	0.363	0.103	0.329
DeepSeek-Math 7B	Text-only (LoRA)	0.463	0.287	0.176	0.362	0.369	0.738
	COMPOSE (ours)	0.525	0.285	0.240	0.429	0.508	0.808

cluster of relevant future papers than to unrelated papers. Text-only and Prompt-only produce text broadly similar to future papers (Tgt-Sim 0.463 and 0.471), but their Neg-Sim is also high, yielding smaller Gaps (0.176 and 0.174) and weaker retrieval. This suggests that, without graph conditioning, these models capture the right topic but fail to isolate the specific future result. **COMPOSE** achieves the highest H@10 (0.508) and H@100 (0.808), reflecting that its generated text ranks the correct future paper higher across the 47K pool than any other variant. **COMPOSE** also leads on NMCP Precision (0.560) and Match (0.730), confirming that its outputs align with future theorems at the formal and informal level, not just topically. The same pattern holds with the Mistral 7B decoder, where we consistently lead on all metrics, demonstrating the significant signal provided by our dual-graph conditioning.

Table 2 compares against external baselines on the same test set, where differences between models are sharpest. **COMPOSE** achieves the largest Gap (0.240) and the highest Exp-Sim (0.429), confirming that its outputs are not only closer to the specific target paper but also to the broader set of papers sharing the same citation context. While the other models achieve high Tgt-Sim, their Neg-Sim is equally high, meaning they capture the right topic but fail to isolate the specific future result. **COMPOSE** ranks the correct future papers in the top 10 in 50.8%, outperforming all baselines. GIANTS performs worse on retrieval because its summarization-style outputs stay closer to the broader cluster than to the specific target paper. As shown in Figure 3, **COMPOSE** consistently dominates across all Hits@K.

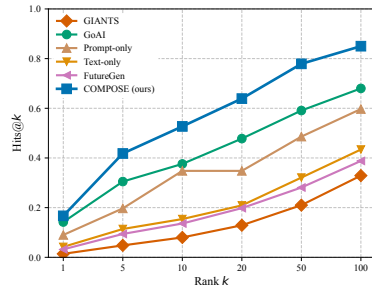


Figure 3: Hit@k comparison across models from $k = 1$ to 100.

As shown in Figure 3, **COMPOSE** consistently dominates across all Hits@K.

4.3 LLM Judge Evaluation

To complement automatic retrieval metrics, we evaluate generation quality with a pre-2024 GPT model as an LLM judge (see Table 3). We score each output on five dimensions: Content, Depth, Novelty, Precision, and Specificity. The same judge prompt and scoring are applied uniformly to all compared models (see Appendix D).

COMPOSE (DeepSeek) achieves the highest overall score (3.36/5), leading in Mathematical Content (3.45), Technical Depth (3.52), Precision (3.23), and Specificity (3.52). GIANTS and FutureGen score higher on Novelty because their outputs are broader and less constrained, but lower on Content and Depth because they include less concrete mathematics.

Table 3: LLM judge scores (1-5, higher is better).

Model	Cont.	Depth	Nov.	Prec.	Spec.	Ovrl.
Prompt-only	2.88	3.16	3.21	3.02	3.21	3.10
GOAI-GPT	2.52	2.69	3.24	2.90	3.29	2.93
GIANTS	1.91	2.75	3.27	2.53	3.28	2.75
ResearchAgent-GPT	1.74	2.10	2.86	2.21	2.99	2.38
Text-only (LoRA)	1.86	1.91	2.42	2.04	2.43	2.13
FutureGen	1.40	1.79	2.75	1.85	2.77	2.11
Paper-graph-only	1.59	1.57	1.71	1.46	1.71	1.61
COMPOSE (DeepSeek)	3.45	3.52	3.10	3.23	3.52	3.36

Taken together, these results suggest that graph conditioning improves both mathematical quality and grounding.

4.4 Ablation Study

We evaluate the contribution of each component of our model using the DeepSeek-Math 7B decoder. Table 4 reports results for five ablations: removing one encoder, removing the bidirectional fusion, removing stage-1 pretraining. Each ablation keeps all other components fixed.

Table 4 shows that each major component of COMPOSE contributes to retrieval performance. Removing either encoder causes a drop: without G_s , H@10 falls to 0.135, and without G_f , to 0.390, confirming that both graph modalities contribute complementary signals. Removing bidirectional fusion and stage-1 pretraining further degrades performance, confirming that the scientific and formal graphs provide complementary information. We also achieve the highest Tgt-Sim (0.525) and Gap (0.240), confirming that the full dual-graph model produces text that is not only better ranked but also semantically closer to the correct future paper

Table 4: Ablation study (DeepSeek-Math 7B decoder). Each row removes one component from the full model.

Model	Tgt-Sim	Neg-Sim	Gap	H@10	H@100
Paper-graph-only	0.438	0.274	0.164	0.390	0.695
formal-graph-only	0.347	0.275	0.073	0.135	0.360
w/o fusion	0.367	0.277	0.090	0.195	0.530
w/o stage 1	0.352	0.260	0.093	0.240	0.505
COMPOSE (ours)	0.525	0.285	0.240	0.508	0.808

5 Qualitative Analysis

Appendix F presents six winning cases and one failure, with side-by-side model outputs. Across wins, COMPOSE consistently generates text in the correct mathematical subfield while baselines drift to neighbouring but wrong areas, and in several cases a baseline achieves higher embedding similarity yet fails, confirming that dual-graph conditioning is what drives to correct placement.

6 Limitations and Future Work

Our method relies on approximate informal-formal alignment, which introduces noise into the formal graph encoder. More importantly, generated claims are not verified by a proof assistant, so retrieval and LLM-based evaluation remain proxy signals rather than direct tests of formal correctness. In addition, the benchmark depends on automatically identifying a main claim from each future paper, which may be noisy for papers with multiple results or less standardized theorem statements.

A natural next direction is to incorporate proof-aware verification so that generated claims can be checked directly against a proof assistant. This framework could also support iterative conjecture generation and proof attempts.

7 Conclusion

We introduced grounded future mathematical generation, a task that combines scientific citation context with formal theorem structure to generate future mathematical claims. To support this setting, we constructed a paired scientific-formal dataset and a temporally grounded benchmark over 47K future papers, and proposed COMPOSE, a dual-graph framework for graph-conditioned generation.

Experiments show that COMPOSE produces outputs more similar to real future claims than the baselines do, and LLM-judge evaluation supports this finding. Ablations further show that both graphs are necessary: the scientific graph identifies relevant research directions, while the formal graph keeps predictions grounded in valid mathematical dependencies.

References

- Alex A. Alemi, Francois Chollet, Niklas Een, Geoffrey Irving, Christian Szegedy, and Josef Urban. Deepmath - deep sequence models for premise selection, 2017. URL <https://arxiv.org/abs/1606.04442>.
- Yousef Alhessi, Sólrún Halla Einarsdóttir, George Granberry, Emily First, Moa Johansson, Sorin Lerner, and Nicholas Smallbone. Lemmanaid: Neuro-symbolic lemma conjecturing, 2026. URL <https://arxiv.org/abs/2504.04942>.
- Chenxin An, Ming Zhong, Yiran Chen, Danqing Wang, Xipeng Qiu, and Xuanjing Huang. Enhancing scientific papers summarization with citation graph, 2021. URL <https://arxiv.org/abs/2104.03057>.
- Zhangir Azerbayev, Bartosz Piotrowski, Hailey Schoelkopf, Edward W. Ayers, Dragomir Radev, and Jeremy Avigad. Proofnet: Autoformalizing and formally proving undergraduate-level mathematics, 2023. URL <https://arxiv.org/abs/2302.12433>.
- Ibrahim Al Azher, Miftahul Jannat Mokarrama, Zhishuai Guo, Sagnik Ray Choudhury, and Hamed Alhoori. Futuregen: A rag-based approach to generate the future work of scientific article, 2025. URL <https://arxiv.org/abs/2503.16561>.
- Jinheon Baek, Sujay Kumar Jauhar, Silviu Cucerzan, and Sung Ju Hwang. Researchagent: Iterative research idea generation over scientific literature with large language models, 2025. URL <https://arxiv.org/abs/2404.07738>.
- Bruno Barras, Samuel Boutin, Cristina Cornes, Judicaël Courant, Yann Coscoy, David Delahaye, Daniel de Rauglaudre, Jean-Christophe Filliâtre, Eduardo Giménez, Hugo Herbelin, et al. The coq proof assistant reference manual. *INRIA, version*, 6(11):17–21, 1999.
- Rafael Cabral, Tuan Manh Do, Xuejun Yu, Wai Ming Tai, Zijin Feng, and Xin Shen. Proofflow: A dependency graph approach to faithful proof autoformalization, 2025. URL <https://arxiv.org/abs/2510.15981>.
- Alex Davies, Petar Veličković, Lars Buesing, Sam Blackwell, Daniel Zheng, Nenad Tomašev, Richard Tanburn, Peter Battaglia, Charles Blundell, András Juhász, Marc Lackenby, Geordie Williamson, Demis Hassabis, and Pushmeet Kohli. Advancing mathematics by guiding human intuition with AI. *Nature*, 600(7887):70–74, 2021. doi: 10.1038/s41586-021-04086-x.
- Kefan Dong and Tengyu Ma. Stp: Self-play llm theorem provers with iterative conjecturing and proving, 2025. URL <https://arxiv.org/abs/2502.00212>.
- Emily First, Markus N. Rabe, Talia Ringer, and Yuriy Brun. Baldur: Whole-proof generation and repair with large language models, 2023. URL <https://arxiv.org/abs/2303.04910>.
- Guoxiong Gao, Haocheng Ju, Jiedong Jiang, Zihan Qin, and Bin Dong. A semantic search engine for mathlib4. In *Findings of the Association for Computational Linguistics: EMNLP 2024*, pages 8001–8013, 2024a.
- Guoxiong Gao, Haocheng Ju, Jiedong Jiang, Zihan Qin, and Bin Dong. A semantic search engine for mathlib4. 2024b. URL <https://arxiv.org/abs/2403.13310>.
- Xian Gao, Zongyun Zhang, Ting Liu, and Yuzhuo Fu. Goai: Enhancing ai students’ learning paths and idea generation via graph of ai ideas, 2025. URL <https://arxiv.org/abs/2503.08549>.
- Justin Gilmer, Samuel S. Schoenholz, Patrick F. Riley, Oriol Vinyals, and George E. Dahl. Neural message passing for quantum chemistry, 2017. URL <https://arxiv.org/abs/1704.01212>.

- Joy He-Yueya, Anikait Singh, Ge Gao, Michael Y. Li, Sherry Yang, Chelsea Finn, Emma Brunskill, and Noah D. Goodman. Giants: Generative insight anticipation from scientific literature, 2026. URL <https://arxiv.org/abs/2604.09793>.
- Edward J. Hu, Yelong Shen, Phillip Wallis, Zeyuan Allen-Zhu, Yuanzhi Li, Shean Wang, Lu Wang, and Weizhu Chen. Lora: Low-rank adaptation of large language models, 2021. URL <https://arxiv.org/abs/2106.09685>.
- Prithwish Jana, Kaan Kale, Ahmet Ege Tanriverdi, Cruise Song, Sriram Vishwanath, and Vijay Ganesh. ProofBridge: Auto-Formalization of Natural Language Proofs in Lean via Joint Embeddings. In *Proceedings of the 14th International Conference on Learning Representations (ICLR)*, 2026. arXiv:2510.15681.
- Albert Q. Jiang, Sean Welleck, Jin Peng Zhou, Wenda Li, Jiacheng Liu, Mateja Jamnik, Timothée Lacroix, Yuhuai Wu, and Guillaume Lample. Draft, sketch, and prove: Guiding formal theorem provers with informal proofs, 2023. URL <https://arxiv.org/abs/2210.12283>.
- Kazumi Kasaura, Naoto Onda, Yuta Oriike, Masaya Taniguchi, Akiyoshi Sannai, and Sho Sonoda. Discovering new theorems via llms with in-context proof learning in lean, 2025. URL <https://arxiv.org/abs/2509.14274>.
- Imre Lakatos. *Proofs and Refutations: The Logic of Mathematical Discovery*. Cambridge University Press, 1976.
- Zhaoyu Li, Jialiang Sun, Logan Murphy, Qidong Su, Zenan Li, Xian Zhang, Kaiyu Yang, and Xujie Si. A survey on deep learning for theorem proving, 2024. URL <https://arxiv.org/abs/2404.09939>.
- Xinyu Liu, Zixuan Xie, Amir Moeini, Claire Chen, Shuze Daniel Liu, Yu Meng, Aidong Zhang, and Shangtong Zhang. Mathliblemma: Folklore lemma generation and benchmark for formal mathematics, 2026. URL <https://arxiv.org/abs/2602.02561>.
- Kyle Lo, Lucy Lu Wang, Mark Neumann, Rodney Kinney, and Dan S. Weld. S2orc: The semantic scholar open research corpus, 2020. URL <https://arxiv.org/abs/1911.02782>.
- Chris Lu, Cong Lu, Robert Tjarko Lange, Jakob Foerster, Jeff Clune, and David Ha. The ai scientist: Towards fully automated open-ended scientific discovery, 2024a. URL <https://arxiv.org/abs/2408.06292>.
- Jianqiao Lu, Yingjia Wan, Zhengying Liu, Yinya Huang, Jing Xiong, Chengwu Liu, Jianhao Shen, Hui Jin, Jipeng Zhang, Haiming Wang, Zhicheng Yang, Jing Tang, and Zhijiang Guo. Process-driven autoformalization in lean 4, 2024b. URL <https://arxiv.org/abs/2406.01940>.
- The mathlib Community. The lean mathematical library. In *Proceedings of the 9th ACM SIGPLAN International Conference on Certified Programs and Proofs, POPL '20*, page 367–381. ACM, January 2020. doi: 10.1145/3372885.3373824. URL <http://dx.doi.org/10.1145/3372885.3373824>.
- Maciej Mikula, Szymon Tworkowski, Szymon Antoniak, Bartosz Piotrowski, Albert Qiaochu Jiang, Jin Peng Zhou, Christian Szegedy, Łukasz Kuciński, Piotr Miłoś, and Yuhuai Wu. Magnushammer: A transformer-based approach to premise selection, 2024. URL <https://arxiv.org/abs/2303.04488>.
- Naoto Onda, Kazumi Kasaura, Yuta Oriike, Masaya Taniguchi, Akiyoshi Sannai, and Sho Sonoda. Lean-conjecturer: Automatic generation of mathematical conjectures for theorem proving, 2025. URL <https://arxiv.org/abs/2506.22005>.
- Lawrence C Paulson. *Isabelle: A generic theorem prover*. Springer, 1994.
- Marissa Radensky, Simra Shahid, Raymond Fok, Pao Siangliulue, Tom Hope, and Daniel S. Weld. Human-llm compound system for scientific ideation through facet recombination and novelty evaluation, 2026. URL <https://arxiv.org/abs/2409.14634>.
- Piotr Rudnicki. An overview of the mizar project. In *Proceedings of the 1992 Workshop on Types for Proofs and Programs*, pages 311–330, 1992.
- Zhihong Shao, Peiyi Wang, Qihao Zhu, Runxin Xu, Junxiao Song, Xiao Bi, Haowei Zhang, Mingchuan Zhang, Y. K. Li, Y. Wu, and Daya Guo. Deepseekmath: Pushing the limits of mathematical reasoning in open language models, 2024. URL <https://arxiv.org/abs/2402.03300>.
- Chenglei Si, Diyi Yang, and Tatsunori Hashimoto. Can llms generate novel research ideas? a large-scale human study with 100+ nlp researchers, 2024. URL <https://arxiv.org/abs/2409.04109>.

- Elif Uskuplu, Lawrence S. Moss, and Valeria de Paiva. Knowtex: Visualizing mathematical dependencies, 2025. URL <https://arxiv.org/abs/2601.15294>.
- Aaron van den Oord, Yazhe Li, and Oriol Vinyals. Representation learning with contrastive predictive coding, 2019. URL <https://arxiv.org/abs/1807.03748>.
- Haiming Wang, Mert Unsal, Xiaohan Lin, Mantas Baksys, Junqi Liu, Marco Dos Santos, Flood Sung, Marina Vinyes, Zhenzhe Ying, Zekai Zhu, Jianqiao Lu, Hugues de Saxcé, Bolton Bailey, Chendong Song, Chenjun Xiao, Dehao Zhang, Ebony Zhang, Frederick Pu, Han Zhu, Jiawei Liu, Jonas Bayer, Julien Michel, Longhui Yu, Léo Dreyfus-Schmidt, Lewis Tunstall, Luigi Pagani, Moreira Machado, Pauline Bourigault, Ran Wang, Stanislas Polu, Thibaut Barroyer, Wen-Ding Li, Yazhe Niu, Yann Fleureau, Yangyang Hu, Zhouliang Yu, Zihan Wang, Zhilin Yang, Zhengying Liu, and Jia Li. Kimina-prover preview: Towards large formal reasoning models with reinforcement learning, 2025a. URL <https://arxiv.org/abs/2504.11354>.
- Hanyu Wang, Ruohan Xie, Yutong Wang, Guoxiong Gao, Xintao Yu, and Bin Dong. Aria: An agent for retrieval and iterative auto-formalization via dependency graph, 2025b. URL <https://arxiv.org/abs/2510.04520>.
- Heng Wang, Pengcheng Jiang, Jiashuo Sun, Zhiyi Shi, Haofei Yu, Jiawei Han, and Heng Ji. Learning to predict future-aligned research proposals with language models, 2026. URL <https://arxiv.org/abs/2603.27146>.
- Liang Wang, Nan Yang, Xiaolong Huang, Binxing Jiao, Linjun Yang, Daxin Jiang, Rangan Majumder, and Furu Wei. Text embeddings by weakly-supervised contrastive pre-training, 2024a. URL <https://arxiv.org/abs/2212.03533>.
- Mingzhe Wang, Yihe Tang, Jian Wang, and Jia Deng. Premise selection for theorem proving by deep graph embedding, 2017. URL <https://arxiv.org/abs/1709.09994>.
- Qingyun Wang, Doug Downey, Heng Ji, and Tom Hope. Scimon: Scientific inspiration machines optimized for novelty. In *Proceedings of the 62nd Annual Meeting of the Association for Computational Linguistics (Volume 1: Long Papers)*, page 279–299. Association for Computational Linguistics, 2024b. doi: 10.18653/v1/2024.acl-long.18. URL <http://dx.doi.org/10.18653/v1/2024.acl-long.18>.
- Yuhuai Wu, Albert Q. Jiang, Wenda Li, Markus N. Rabe, Charles Staats, Mateja Jamnik, and Christian Szegedy. Autoformalization with large language models, 2022. URL <https://arxiv.org/abs/2205.12615>.
- Huajian Xin, Daya Guo, Zhihong Shao, Zhizhou Ren, Qihao Zhu, Bo Liu, Chong Ruan, Wenda Li, and Xiaodan Liang. Deepseek-prover: Advancing theorem proving in llms through large-scale synthetic data, 2024. URL <https://arxiv.org/abs/2405.14333>.
- Guangzhi Xiong, Eric Xie, Amir Hassan Shariatmadari, Sikun Guo, Stefan Bekiranov, and Aidong Zhang. Improving scientific hypothesis generation with knowledge grounded large language models, 2024. URL <https://arxiv.org/abs/2411.02382>.
- Kaiyu Yang, Aidan Swope, Alex Gu, Rahul Chalamala, Peiyang Song, Shixing Yu, Saad Godil, Ryan Prenger, and Anima Anandkumar. LeanDojo: Theorem proving with retrieval-augmented language models. In *Neural Information Processing Systems (NeurIPS)*, 2023.
- Lan Zhang, Marco Valentino, and Andre Freitas. Autoformalization in the wild: Assessing llms on real-world mathematical definitions, 2025. URL <https://arxiv.org/abs/2502.12065>.
- Thomas Zhu, Pietro Monticone, Jeremy Avigad, and Sean Welleck. Leanarchitect: Automating blueprint generation for humans and ai, 2026. URL <https://arxiv.org/abs/2601.22554>.

A Dataset Construction Details

Table 5 summarizes the distribution of papers across mathematical domains in our dataset. The dataset includes papers published between 2000 and 2023.

Table 5: Dataset statistics by mathematical domain.

Domain	# Papers
Probability	119,644
Algebraic Geometry	113,360
Analysis	104,483
Mathematical Physics	43,035
Representation Theory	42,720
Dynamical Systems	39,153
Differential Geometry	34,138
Combinatorics	27,220
Total (all domains)	520,773

A.1 Citation Subgraph Construction

Starting from the anchor paper, we follow outgoing citation edges hop by hop. We retain up to 5 cited papers at the first hop and up to 3 cited papers per node for the last hops. Candidate neighbors are ranked by citation-context relevance rather than sampled uniformly. Nodes without publication year metadata are discarded. Each paper node is represented by its abstract, encoded with E5-large-v2 Wang et al. [2024a].

Since not all citations are equally informative, we rank candidate neighbors at each expansion step relative to the current paper node. The ranking uses citation-context heuristics intended to capture relevance to the surrounding scientific development, including appearances in the abstract, introduction, main result claim, or proof-related passages; explicit dependency cues such as “using,” “by,” or “follows from”; repeated technical mentions; and proximity to extracted theorem. At each hop, we retain only the top-k candidates, yielding a compact citation subgraph that preserves the most relevant local scientific context.

A.1.1 Citation Relevance Selection: Illustrative Example

To illustrate the difference between relevant and peripheral citations, we show two citations from the same paper (ArXiv:1911.06307, Grifo-Ma-Schwede) and explain why one is selected as a neighbor and the other is not.

High-relevance citation. *“arXiv:1702.06876, Grifo-Huneke”* This paper is cited throughout the introduction and proof sections with explicit dependency cues. For example: *“In prime characteristic p , Grifo and Huneke [GH19] showed that Harbourne’s conjecture holds for ideals defining F -pure rings”, “the theorem above extends [GH19, Theorem 3.2 and Theorem 4.1]”, and “The containment $Q^{\binom{h-1}{n-1}+1} \subseteq Q^n$ for all $n \geq 1$ now follows by induction on n , as in [GH19, Theorem 4.1]”*. The paper’s main results are direct extensions of this work, and specific lemmas are invoked repeatedly in proofs.

Low-relevance citation (not selected). *“Birational geometry of algebraic varieties” (Kollár-Mori)*. This work does not appear anywhere in the body of the paper — it appears only in the citation subgraph through indirect bibliographic links. It is not cited in the introduction, proofs, or any technical passage, and has no connection to the symbolic power containment results developed in the paper.

Citations that appear repeatedly in proof-related passages with explicit dependency language (“extends [X]”, “as in [X, Lemma Y]”, “follows from [X]”) score significantly higher than works that appear only through indirect bibliographic links with no direct textual dependency. This ensures the subgraph captures the papers that directly shaped the mathematical content of the target paper.

A.2 Proof-Flow Graph Extraction

For papers within the first two citation hops, we extract a proof-flow graph from the full text. We identify theorem nodes corresponding to five types: *theorem*, *lemma*, *proposition*, *corollary*, and *definition*. Directed edges are added between theorem nodes when the text contains explicit dependency references, detected with regular expressions matching patterns such as “by Lemma 2.1” or “using Theorem 3.4”. We filter out malformed statement spans, including nodes that begin mid-sentence. Papers with fewer than three valid theorem nodes after filtering are discarded. The resulting graph is a directed acyclic graph that approximates the proof-flow structure of the paper.

A.3 Formal Graph Construction

The matched theorem serves as the root of a local dependency subgraph extracted from Mathlib, where nodes are formal Lean theorems and edges capture dependency relations between them. We expand this subgraph up to 3 hops from the root, yielding between 8 and 15 theorems per sample.

A.4 Informal-to-Formal Alignment

Table 6: Number of extracted theorems and high-confidence Mathlib matches (cosine ≥ 0.84) per mathematical domain.

Domain	Extracted Theorems	Matched Theorems
Probability	38,499	8,846
Algebraic Geometry	53,118	5,779
Analysis	40,650	9,534
Mathematical Physics	26,864	3,974
Representation Theory	21,836	3,263
Dynamical Systems	25,312	4,137
Differential Geometry	32,326	2,652
Combinatorics	38,690	5,325
Other	435,553	76,915
Total	712,848	120,425

Bridging informal mathematical text and formal Lean theorems is challenging because of the gap between natural mathematical language and formal library theorems. To understand which alignment strategy is most effective, we compare three methods. The first is Autoformalization, which translates an informal theorem into a Lean-style formal stub before retrieval. The second is informal-to-formal retrieval, which avoids generation and retrieves directly from the informal theorem into a space of formal Lean theorem signatures. The third is informal-to-informal retrieval, which avoids the formal surface form by retrieving against natural-language theorem descriptions from FrenzyMath and then mapping the retrieved description back to its corresponding Mathlib theorem.

As shown in Table 7, Autoformalization-based approaches achieve at most 6.1% high-confidence matches, while direct informal-to-formal retrieval performs similarly poorly, confirming that the vocabulary mismatch between informal and formal mathematics is a major bottleneck. In contrast, informal-to-informal retrieval achieves 16.9% high-confidence matches, nearly three times better than the strongest competing method. We therefore adopt this alignment strategy in all downstream experiments.

The "Precision" column in Table 7 is computed by sampling 1000 matched pairs per method, scoring them with an LLM judge, and reporting the resulting percentage. The full prompt is shown in Figure 4.

Table 8 shows the coverage precision tradeoff as the threshold τ varies for the adopted E5-MISTRAL \rightarrow FrenzyMath method.

Table 7: Comparison of alignment strategies for matching clean informal paper theorems to Mathlib theorems. Coverage: % of statements with any match. High-conf.: % of statements with cosine similarity ≥ 0.84 . Precision: % of high-confidence matches judged as related or better by an LLM judge on 1000 sampled pairs.

Strategy	Method	Coverage(%)	High-conf. (%)	Precision (%)
Autoformalization	Kimina-7B \rightarrow BM25	23.0%	0.4%	0.0%
	Kimina-7B \rightarrow namespace	25.0%	0.1%	0.5%
	Kimina-7B \rightarrow Lean sig.	100%	5.9%	7.0%
	Gemini-3 \rightarrow BM25	99.4%	6.1%	—
Informal \rightarrow Formal	Keyword \rightarrow BM25	99%	0.2%	2.0%
	e5-large \rightarrow Lean sig.	100%	8.7%	1.5%
	e5-mistral \rightarrow Lean sig.	100%	6.2%	45.4%
Informal \rightarrow Informal	BM25 \rightarrow FrenzyMath	100%	1.2%	7.7%
	e5-large \rightarrow FrenzyMath	100%	3.4%	26.1%
	e5-mistral \rightarrow FrenzyMath (ours)	100%	16.9%	66.1%

Table 8: Coverage and precision for the E5-MISTRAL \rightarrow FrenzyMath alignment pipeline as a function threshold τ . The row at $\tau = 0.84$ is the operating point used in our experiments.

τ	High-conf. (%)	precision (%)
0.70	45.2	31.0
0.75	32.1	42.5
0.80	24.3	55.8
0.84	16.9	66.1
0.88	10.1	78.3
0.92	4.2	88.0

A.4.1 Alignment Retrieval Details

We describe the retrieval implementation for each method in Table 7. Autoformalization and informal-to-formal methods retrieve from the Mathlib corpus theorems indexed by their Lean 4 signatures. High-confidence matches are defined as cosine similarity ≥ 0.84 between the paper theorem and the retrieved Mathlib theorem.

Autoformalization. Each informal paper theorem is first translated into a Lean 4 formal stub using either Kimina-7B [Wang et al., 2025a] or Gemini-2.5-Flash, prompted with five in-context examples. The prompt is shown in Figure A.4.1. Three retrieval strategies are then applied to the generated stub:

- **BM25 retrieval.** We build a BM25 index over Mathlib theorem names concatenated with their Lean 4 signatures. We retrieve the top-5 results with a minimum BM25 score of 5.
- **Namespace matching.** We build a prefix index over all Mathlib theorem names. From the generated stub, we extract identifiers and look up Mathlib theorems whose name shares the longest matching prefix. Results are ranked by prefix specificity, top-5 returned.
- **Dense retrieval.** We embed the informal text as "query: <text>" using e5-large-v2(1024-dim, L2-normalized) and compute cosine similarity against precomputed embeddings of all Mathlib Lean 4 signatures (embedded as "passage: <sig>"). Top-10 by cosine score.

Informal-to-formal retrieval. These methods bypass Autoformalization and retrieve directly from the informal paper theorem text into the space of formal Lean 4 signatures:

- **Keyword \rightarrow BM25.** We tokenize both queries and the Mathlib signature corpus by lower-casing, extracting alphanumeric tokens via regex, and removing a custom stopword list. We build a BM25 index over the tokenized Lean 4 signatures and retrieve the top-5 results with a minimum score of 1.0.

LLM Judge Prompt

You are a mathematical alignment judge. Given an informal theorem from a research paper and a candidate Mathlib (Lean 4) theorem, rate how well the Mathlib theorem aligns with the informal theorem.

Score from 1 to 5:

- 1 = Completely unrelated mathematics
- 2 = Same broad area but different specific topic
- 3 = Related topic, shares key concepts or structures
- 4 = Closely related, formalizes a component or special case of the informal result
- 5 = Direct match, formalizes the same or equivalent result

Respond with only a single digit: 1, 2, 3, 4, or 5.

Informal theorem from paper: {informal}

Candidate Mathlib theorem: {formal}

Figure 4: Prompt used to evaluate alignment quality for the Precision column in Table 7. We use Gemini-2.5-Flash with temperature 0.

- **e5-large** → **Lean sig.** We embed the informal text as "query: <text>" using e5-large-v2 and compute cosine similarity against precomputed embeddings of all Mathlib Lean 4 signatures (embedded as "passage: <sig>"). Top-10 by cosine score.
- **e5-mistral** → **Lean sig.** Same setup but using e5-mistral-7b-instruct with last-token pooling and the instruction prefix "Instruct: Retrieve a Mathlib theorem that formalizes the following mathematical theorem.". Corpus signatures are embedded without instruction prefix. Top-5 by cosine score.

Informal-to-informal retrieval. These methods retrieve against natural-language theorem descriptions from the FrenzyMath dataset, which provides informal names and descriptions for Mathlib theorems. The retrieved description is then mapped back to its corresponding formal Mathlib theorem:

- **BM25** → **FrenzyMath.** We build a BM25 index over Mathlib theorem names concatenated with their Lean 4 signatures. We retrieve the top-5 results with a minimum BM25 score of 5.
- **e5-large** → **FrenzyMath.** We embed informal descriptions from FrenzyMath as "passage: <desc>" with e5-large-v2 (83,807 unique entries) and embed each paper theorem as "query: <text>". Top-5 by cosine similarity.
- **e5-mistral** → **FrenzyMath (ours).** We use e5-mistral-7b-instruct with last-token pooling and the instruct prefix "Instruct: Retrieve a Mathlib theorem that formalizes the following mathematical theorem.". We retrieve the top-5 candidates by cosine similarity.

System: You are an expert in Lean4 and Mathlib. Convert the following mathematical theorem statement into a Lean4 theorem stub using Mathlib.

Rules:

- Use correct Mathlib 4 types and namespaces (e.g. `Fintype.card`, `IsCyclic`, `Nat.Prime`)
- Write only the theorem signature ending with `:= by sorry` or `:= sorry`
- Do NOT write a proof, just the stub
- Use `import Mathlib` and appropriate open statements

[5 in-context examples:]

Text: Let G be a finite cyclic group. Then the exponent of G equals the cardinality of G .

Lean4: `theorem cyclic_exponent_eq_card {G : Type*} [Group G] [Fintype G] [IsCyclic G] :
Monoid.exponent G = Fintype.card G := by exact IsCyclic.exponent_eq_card`

Text: Let p be a prime number. Then a finite group of order p is cyclic.

Lean4: `theorem prime_order_cyclic {G : Type*} [Group G] [Fintype G] {p : ℕ} [hp : Fact p.Prime]
(h : Fintype.card G = p) : IsCyclic G := by exact
isCyclic_of_prime_card h`

Text: Let R be a commutative ring and I an ideal. The degree of the zero element of $R[X]$ is 0.

Lean4: `theorem degreeOf_C_zero {R : Type*} [CommRing R] (x : ℕ) :
MvPolynomial.degreeOf x (0 : MvPolynomial ℕ R) = 0 := by simp
[MvPolynomial.degreeOf_C]`

Text: If f is `ContDiff` of order n , then for any polynomial p , $x \mapsto p(x^{-1}) \cdot \text{expNegInvGlue}(x)$ is also `ContDiff` of order n .

Lean4: `theorem contDiff_poly_inv_glue {n : ℕ∞} (p : ℝ[X]) :
ContDiff ℝ n (fun x ↦ p.eval x⁻¹ * expNegInvGlue x) :=
expNegInvGlue.contDiff_polynomial_eval_inv_mul p`

Text: Let G be a finite group with normal subgroup N s.t. G/N is a Frobenius group with cyclic complement. If $|F|$ and $|N|$ are coprime, then some prime divides $|G|$.

Lean4: `theorem frobenius_prime_divisor {G : Type*} [Group G] [Fintype G]
{N : Subgroup G} (hN : N.Normal) (hC : IsCyclic (G / N))
(hcard : Nat.Coprime (Fintype.card N) (Fintype.card (G / N))) :
∃ p : ℕ, Nat.Prime p ∧ p | Fintype.card G := by
exact ⟨_, Nat.minFac_prime (Fintype.card_pos.ne'), Nat.minFac_dvd _⟩`

Text: *{informal_theorem}*

Lean4: *[generated stub]*

Figure 5: Few-shot prompt used for autoformalization (Gemini-2.0-Flash). The generated Lean 4 stub is used as a query for BM25 namespace, and dense retrieval against Mathlib.

A.5 Training Target Types

We use the same target-construction pipeline for both the training dataset and the future-paper retrieval benchmark. For each paper, we first try to extract its main mathematical claim from the body text using a set of heuristics, including regular-expression matching for phrases such as “we prove,” “we show,” “Main Theorem,” and early numbered theorem statements. When no single main claim can be identified reliably, we fall back to alternative targets such as the abstract or a supporting theorem with clear local context. This yields a consistent target-construction process across both training and evaluation, while handling different ways of stating the main claim.

Each training sample is paired with several target types derived from the same graph. These targets expose the model to different forms of mathematical output from the same underlying context, helping it learn richer graph representations instead of specializing to a single output style.

A **Claim** is the main mathematical result of the paper, extracted from sentences beginning with “we prove,” “we show,” or identified as Theorem 1 or Main Theorem in the text. An **Abstract** target is the full paper abstract. A **Lemma in claim** is a supporting lemma together with the neighboring theorems it depends on, providing local proof flow context. **Lean only** targets consist of the formal

Lean signatures of the matched Mathlib theorems, and **Informal + Lean** combines the informal claim with those signatures. Training on this mixture encourages the model to learn graph representations that generalize across output types, which benefits Claim generation at evaluation time.

Table 9 shows the distribution across target types in the final dataset.

Table 9: Training target types and sample counts in the final dataset.

Target Type	Samples
Abstract	12,156
Claim	33,846
Claim + proof flow	14,423
Lemma in claim	42,517
Lean only	2,817
Informal + Lean	2,817
Total	108,576

A.6 Illustrative Example

We illustrate the full structure of one training sample from the dataset.

Target paper. ArXiv:1911.06307 (Grifo-Ma-Schwede) — symbolic power containments in singular rings in positive characteristic.

Target statement (claim).

Let R be an F -finite Gorenstein ring of prime characteristic p and $Q \subseteq R$ an ideal of finite projective dimension with big height h . If R/Q is F -pure, then $Q^{(hn-h+1)} \subseteq Q^n$ for all $n \geq 1$. If R/Q is strongly F -regular and $h \geq 2$, then $Q^{((h-1)(n-1)+1)} \subseteq Q^n$ for all $n \geq 1$.

Citation subgraph (7 paper nodes, 6 edges). The citation subgraph retains the 7 highest-relevance cited papers, selected by citation-context relevance as described in Appendix A.1:

- Hochster-Huneke: Comparison of symbolic and ordinary powers of ideals (2002) cited 10 times, invoked in proofs as “by [HH02, Lemma 2.2]” and “by [HH02, Lemma 2.4]”
- Grifo-Huneke: Symbolic powers of ideals defining F -pure and strongly F -regular rings (2019) — cited 9 times, main results are direct extensions: “the theorem above extends [GH19, Theorem 3.2 and Theorem 4.1]”
- Takagi: Formulas for multiplier ideals on singular varieties (2006) cited 10 times, specific lemmas invoked: “by [Tak06, Theorem 4.6]”, “follows from [Tak06, Lemma 4.5]”
- Fedder: F -purity and rational singularity (1983) cited 6 times, the Fedder criterion is a central tool: “c.f. [Fed83, Corollaries to Lemma 1.6]”
- Peskine-Szpiro: Dimension projective finie et cohomologie locale (1973) cited in proof: “By [PS73, Théorème (I.7)]”
- Takagi-Yoshida: Generalized test ideals and symbolic powers (2008) cited 4 times with specific result: “extends [TY08, Remark 3.4]”
- Glassbrenner: Strongly F -regularity in images of regular rings (1996) cited 3 times, criterion extended: “extends [Gla96]”

Directed citation edges connect the anchor paper to each of these works; Grifo-Huneke (2019) is additionally connected to Hochster-Huneke (2002), reflecting the citation chain within the subgraph.

Proof-flow graph of the anchor paper (10 nodes, 7 edges). Statement nodes extracted from the paper text, with dependency edges detected from explicit references:

- **[definition]** Definition 2.3: The Frobenius non-splitting ideal $I^e(Q)$ for an ideal Q in an F -finite ring R .
- **[lemma]** Lemma 2.6: $\text{Ass}(R/I^e(Q)) \subseteq \text{Ass}(R/Q)$ for all $e > 0$; equality holds when R is F -pure.
- **[lemma]** Lemma 2.9: For $q = p^e$, $Q^{(q(h+n-1)-h+1)} \subseteq I^e(Q^{(n)})$.
- **[lemma]** Lemma 3.1: Any map $\phi \in \text{Hom}_{R/Q}(F_*^e(R/Q), R/Q)$ lifts to $\tilde{\phi} \in \text{Hom}_R(F_*^e R, R)$.
- **[theorem]** Theorem 3.11 (Main): $Q^{(hn-h+1)} \subseteq Q^n$ for F -pure rings; $Q^{((h-1)(n-1)+1)} \subseteq Q^n$ for strongly F -regular rings.

Dependency edges: Theorem 3.11 \rightarrow Lemma 3.1, Theorem 3.11 \rightarrow Lemma 2.9, Lemma 2.9 \rightarrow Lemma 2.6, Lemma 3.1 \rightarrow Definition 2.3.

Mathlib theorem subgraph (10 nodes, 8 edges). The formal subgraph is anchored at `Ideal.pow_le_pow_left`, the Mathlib theorem stating $I^m \leq I^n$ whenever $I \leq J$ or $m \geq n$, which is the closest formal counterpart to the symbolic power containment result. The subgraph expands through its proof dependencies:

- `Ideal.pow_le_pow_left`: $\forall (h : I \leq J), I^n \leq J^n$
- `Ideal.pow_le_pow_right`: $\forall (h : m \leq n), I^n \leq I^m$
- `Ideal.mul_le_left`: $I \cdot J \leq I$
- `Ideal.span_pow_le_pow`: *containment of span under power*
- `Ideal.IsPrime.mul_mem_iff_mem_or_mem`: $x \cdot y \in P \Rightarrow x \in P \vee y \in P$
- `Ideal.mem_pow_eq_zero_iff`: *membership criterion in nilradical powers*
- `le_trans`: $a \leq b \rightarrow b \leq c \rightarrow a \leq c$
- `Ideal.span_le`: $\text{span}(s) \leq I \leftrightarrow s \subseteq I$

Dependency edges: `Ideal.pow_le_pow_left` \rightarrow `Ideal.mul_le_left`, `Ideal.pow_le_pow_left` \rightarrow `le_trans`, `Ideal.pow_le_pow_right` \rightarrow `le_trans`, `Ideal.IsPrime.mul_mem_iff_mem_or_mem` \rightarrow `Ideal.span_le`.

B GNN Architecture Details

Both GNN encoders use the same architecture with separate parameters. Each encoder consists of $L = 2$ message-passing layers with hidden dimension $d = 1024$. At each layer ℓ , incoming and outgoing neighbor messages are mean-pooled separately and summed to produce an aggregated message $\mathbf{m}_i^{(\ell)}$:

$$\mathbf{m}_i^{(\ell)} = \frac{1}{|\mathcal{N}_{\text{in}}(i)|} \sum_{j \in \mathcal{N}_{\text{in}}(i)} \mathbf{h}_j^{(\ell)} + \frac{1}{|\mathcal{N}_{\text{out}}(i)|} \sum_{j \in \mathcal{N}_{\text{out}}(i)} \mathbf{h}_j^{(\ell)}. \quad (9)$$

The message is transformed by a linear layer followed by ReLU activation:

$$\tilde{\mathbf{h}}_i^{(\ell)} = \text{ReLU}\left(\mathbf{W}_{\text{msg}}^{(\ell)} \mathbf{m}_i^{(\ell)}\right). \quad (10)$$

The node state is then updated via a learned scalar gated residual connection:

$$g_i^{(\ell)} = \sigma\left(\mathbf{W}_{\text{gate}}^{(\ell)} \left[\mathbf{h}_i^{(\ell)} \parallel \tilde{\mathbf{h}}_i^{(\ell)}\right]\right), \quad \mathbf{h}_i^{(\ell+1)} = g_i^{(\ell)} \tilde{\mathbf{h}}_i^{(\ell)} + (1 - g_i^{(\ell)}) \mathbf{h}_i^{(\ell)}, \quad (11)$$

followed by layer normalization. After L layers, a final linear projection maps each node to a structural vector of dimension 128, which is concatenated with the frozen text embedding to form the final node representation. Table 10 shows the training hyperparameters.

Table 10: Training hyperparameters and architecture details.

Parameter	Value
<i>Architecture</i>	
Encoder 1 (paper)	E5(output dim 1152)
Encoder 2 (theorem)	DeepSeek-Math finetuned (output dim 4096)
Decoder	DeepSeek-Math-7B-Instruct
Bridge MLP	1152 \rightarrow 2048 \rightarrow 4224
Fused dimension	4224
Fusion cross-attention heads	8
Type embeddings	2×4224 (paper, theorem)
Cross-attention layers	8 (at indices 3,7,11,15,19,23,27,31)
LoRA rank	32
Contrastive projection	4224 \rightarrow 4096
Cross-encoder projection	1024 \rightarrow 128 / 4096 \rightarrow 128
E5 alignment projection	4224 \rightarrow 1024
Gen-text E5 projection	4096 \rightarrow 1024
Gen-text thm_ft projection	4096 \rightarrow 4096
Memory bank size	256
<i>Data & Training</i>	
Training samples	$\sim 80,000$
Batch size	8
Epochs	30
Freeze decoder epochs	0
Precision	float32
GPU	NVIDIA H200 (80 GB)
<i>Optimization</i>	
Optimizer	AdamW
LR (bridge, fusion, type embed)	2×10^{-5}
LR (GNN)	2×10^{-6}
LR (LoRA)	1×10^{-6}
LR (cross-attn K/V)	1×10^{-5}
LR (gates)	1×10^{-5}
LR (decoder after unfreeze)	5×10^{-7}
Weight decay (GNN, bridge, cross-attn)	0.01
Weight decay (LoRA)	0.05
Weight decay (gates)	0.0
Gradient clipping (max norm)	1.0
<i>Loss Weights</i>	
Cross-entropy (CE)	1.0
InfoNCE contrastive (λ_{contr})	0.30
Cross-encoder contrastive (λ_{xcontr})	0.20
Graph margin loss	0.5 (margin = 0.2)
alignment	0.5
Link prediction (freeze phase)	0.4
$\lambda_{\text{alignment}}$ (freeze phase)	1.0
InfoNCE temperature (τ)	0.07

C Extended Evaluation Metrics

Table 11: Generation quality and grounding metrics. Struct. = mathematical structure rate. BERTSc. = BERTScore F1 vs. ground-truth future theorem. ROUGE-L = lexical overlap with ground-truth. Fut-R = ROUGE(gen, future) / ROUGE(gen, input); values >1 indicate forward-looking predictions. Bold = best per group

Decoder	Model	Struct.	BERTSc.	ROUGE-L	Fut-R \uparrow
1.223 DeepSeek-Math 7B	COMPOSE (ours)	0.975	0.840	0.066	
	Paper-graph-only	0.940	0.826	0.053	1.084
	Bag-of-Papers	0.900	0.822	0.046	0.962
	Text-only (LoRA)	0.850	0.807	0.148	2.241
	Prompt-only	0.890	0.777	0.048	0.518
Mistral 7B	COMPOSE (ours)	0.877	0.819	0.050	0.441
	Paper-graph-only	0.644	0.808	0.050	0.625
	Bag-of-Papers	0.851	0.826	0.042	0.480
External DeepSeek-Math 7B	GoAI	0.370	0.771	0.047	0.809
	FutureGen	0.645	0.710	0.048	0.520
	ResearchAgent	0.082	0.648	0.054	0.699
GIANTS	GIANTS	0.165	0.752	0.037	0.314
GPT-4.0	GoAI	0.085	0.821	0.125	1.933
	ResearchAgent	0.640	0.814	0.096	0.968
	CoI	0.080	0.811	0.118	1.449

Table 11 evaluates generation quality across four complementary dimensions. Struct. measures whether outputs contain formal mathematical content. Our model achieves 0.975, indicating that nearly every prediction contains meaningful mathematical content. BERTSc. captures semantic similarity to the ground-truth future theorem; our score of 0.840 is the highest across all methods, confirming that our predictions closely match what was actually published. ROUGE-L measures lexical overlap with the ground-truth, where we lead our decoder group. Fut-R is defined as:

$$\text{Fut-R} = \frac{\text{ROUGE-L}(\hat{y}, y^*)}{\text{ROUGE-L}(\hat{y}, x)} \quad (12)$$

where \hat{y} is the generated text, y^* is the ground-truth future theorem, and x is the input paper context. A value above 1.0 means the model’s output shares more content with the ground-truth future theorem than with the papers it was conditioned on, indicating forward-looking prediction. A value below 1.0 means the model is closer to restating its input than to predicting the future. External baselines such as GIANTS (0.314) and Prompt-only (0.518) fall well below 1.0, indicating that they largely restate known results. Our model achieves 1.223, confirming that it produces more forward-looking predictions.

D LLM Judge Evaluation

The LLM judge is based on five dimensions of mathematical quality: Mathematical Content, Technical Depth, Novelty, Precision, and Specificity.

Mathematical Content measures whether the output contains substantive mathematical statements rather than only prose. Technical Depth measures whether the claims are non-trivial and mathematically meaningful. Novelty measures whether the prediction introduces non-obvious ideas rather than simple restatements. Precision measures whether assumptions, objects, and conclusions are stated clearly and correctly. Specificity measures whether the output gives concrete mathematical details rather than vague high-level descriptions. Together, these scores measure both the mathematical content and the quality of the generated text. We report the average score for each dimension, along

with the overall mean across them. The judge receives the generated prediction together with the input paper context and assigns scores on these five dimensions. The full prompt is shown in Figure 6. We use a GPT-4.0 version released before the benchmark period and apply the same prompt and scoring rubric uniformly to all compared models.

LLM Judge Prompt

You are a strict mathematical reviewer evaluating a generated mathematical research prediction.
IMPORTANT: Evaluate both the mathematical substance and the quality of the prediction. Outputs with real mathematical content should be scored higher than fluent but vague prose, but clarity, precision, and technical quality should also be taken into account.
Input papers context: *[input context]*
Generated prediction: *[generated text]*
 Score each dimension (1-5):

1. **Mathematical Content:** Does the text contain actual mathematics (theorems, lemmas, equations, proofs)? Score 1 if only natural language.
2. **Technical Depth:** Are the mathematical claims non-trivial? Score 1 for surface-level statements.
3. **Novelty:** Does the prediction introduce non-obvious mathematical ideas? Score 1 for trivial restatements.
4. **Precision:** Are specific objects, conditions, and conclusions stated precisely?
5. **Specificity:** How concrete and specific are the claims (named theorems, explicit constants, specific spaces/operators)?

Figure 6: LLM judge prompt for mathematical prediction quality evaluation. The prompt explicitly instructs the judge to prioritize mathematical formalism over natural language fluency.

D.1 Embedding Space Analysis

Raw cosine similarity in mathematical embedding spaces is not a reliable retrieval signal in our setting. As shown in Table 13, different embedding models produce broadly similar Tgt-Neg margins, and no single model consistently outperforms the others. Across embedding models, target and unrelated future papers remain too similar to separate generation methods cleanly. In Table 13, we report results using the DeepSeek-based COMPOSE variant rather than the Mistral variant.

This motivates us to fine-tune a DeepSeek-Math embedding model on the 47K benchmark papers for retrieval evaluation, using a margin-ranking objective that pulls together papers with overlapping citation context and pushes apart unrelated papers. Specifically, positive pairs consist of papers that cite the same anchor paper, while negatives are sampled from unrelated citation groups. The model is trained with a contrastive cross-entropy loss over cosine similarities scaled by temperature $\tau = 0.05$, with 5 negatives per anchor. Table 12 provides additional hyperparameter details.

Table 12: Fine-tuned embedding model hyperparameters.

Hyperparameter	Value
Base model	DeepSeek-Math-7B-Instruct
Fine-tuning method	LoRA
LoRA rank / alpha	16 / 32
LoRA dropout	0.05
Target modules	q_proj, v_proj
Optimizer	AdamW
Learning rate	1×10^{-4}
Weight decay	0.01
Batch size	4 × 4 GPUs
Epochs	2
Training pairs	50,000
Negatives per anchor	5
Temperature (τ)	0.05
Max token length	256
Pooling	Last-token, L2-normalized
Embedding dim	4096

Table 13: Raw cosine similarity to future citing papers across seven embedding models on the 2K test set. μ denotes the mean pairwise similarity among the 47K pool papers. Tgt-Neg margins are uniformly small and no method consistently dominates, motivating the use of a fine-tuned theorem embedding model for retrieval evaluation.

Emb. Model (μ)	Method	Tgt-Sim	Neg-Sim	Tgt-Neg	Med. Tgt
DeepSeek-Math-7B ($\mu=0.44$)	COMPOSE (ours)	0.542	0.418	0.124	0.607
	Text-only	0.570	0.441	0.129	0.590
	Bag-of-Papers	0.523	0.399	0.123	0.589
	GIANTS	0.425	0.304	0.121	0.439
	GOAI	0.562	0.441	0.121	0.554
	FutureGen	0.465	0.349	0.115	0.449
	ResearchAgent	0.211	0.199	0.012	0.211
	Prompt-only	0.403	0.297	0.106	0.419
E5-Mistral-7B ($\mu=0.43$)	COMPOSE (ours)	0.535	0.412	0.124	0.652
	Text-only	0.476	0.359	0.117	0.377
	Bag-of-Papers	0.341	0.256	0.085	0.331
	GIANTS	0.534	0.388	0.146	0.659
	GOAI	0.586	0.440	0.146	0.725
	FutureGen	0.383	0.267	0.117	0.318
	ResearchAgent	0.238	0.221	0.017	0.216
	Prompt-only	0.529	0.385	0.145	0.640
Kimina-7B ($\mu=0.64$)	COMPOSE (ours)	0.492	0.479	0.012	0.487
	Text-only	0.472	0.457	0.016	0.481
	Bag-of-Papers	0.487	0.472	0.015	0.482
	GIANTS	0.438	0.417	0.021	0.441
	GOAI	0.375	0.347	0.028	0.367
	FutureGen	0.371	0.357	0.014	0.384
	ResearchAgent	0.452	0.436	0.017	0.452
	Prompt-only	0.418	0.397	0.021	0.416
DeepSeek-Prover -7B ($\mu=0.87$)	COMPOSE (ours)	0.873	0.869	0.003	0.896
	Text-only	0.832	0.826	0.006	0.858
	Bag-of-Papers	0.847	0.842	0.006	0.886
	GIANTS	0.812	0.803	0.009	0.828
	GOAI	0.797	0.789	0.007	0.830
	FutureGen	0.817	0.811	0.006	0.835
	ResearchAgent	0.814	0.806	0.008	0.828
	Prompt-only	0.824	0.816	0.008	0.843
Llemma-7B ($\mu=0.33$)	COMPOSE (ours)	0.338	0.335	0.002	0.343
	Text-only	0.333	0.328	0.005	0.340
	Bag-of-Papers	0.320	0.314	0.006	0.327
	GIANTS	0.301	0.291	0.010	0.319
	GOAI	0.345	0.336	0.010	0.351
	FutureGen	0.312	0.302	0.010	0.320
	ResearchAgent	0.310	0.305	0.006	0.331
	Prompt-only	0.297	0.287	0.011	0.314
Mathstral-7B ($\mu=0.15$)	COMPOSE (ours)	0.154	0.148	0.006	0.157
	Text-only	0.165	0.160	0.006	0.163
	Bag-of-Papers	0.150	0.140	0.010	0.155
	GIANTS	0.092	0.078	0.014	0.094
	GOAI	0.166	0.155	0.012	0.172
	FutureGen	0.135	0.122	0.013	0.135
	ResearchAgent	0.091	0.081	0.010	0.093
	Prompt-only	0.101	0.085	0.016	0.109

E Prompt Templates

We show the exact input and a real generated output for each method on the same example subgraph. for the external baseline we use there code.

For all the external baseline we use the same prompt as mation in ther papre.

COMPOSE (Ours)

Text input (decoder self-attention):
[INST] Title: Discrete Polymatroids
Using the provided paper context, predict the paper’s main mathematical result. [/INST]

Graph inputs (cross-attention, not text):
 G_s : 8 citation subgraph node embeddings $\xrightarrow{\text{GNN}}$ K/V injected at decoder layers 7, 15, 23, 31
 G_f : 10 Mathlib formal subgraph node embeddings $\xrightarrow{\text{GNN}}$ K/V injected at decoder layers 7, 15, 23, 31

Generated output:
In a paper proving that any non-increasing function of non-negative integers is the normalized depth function of some squarefree monomial ideal, a key step is: **Proposition 2.4:** Let S be a simplicial complex and let $K \subset J(S)$ be a vertex k -coloring. Then colorings with no monochromatic components can be obtained by applying one of the following operations iteratively to any coloring C whose complement graph G_C is connected.

Figure 7: COMPOSE (Ours): the decoder receives only the anchor paper title as text; the citation and formal graphs are injected silently via cross-attention.

Text-Only (LoRA)

Input:
[INST] You are a mathematician. Given a paper and related work, predict the paper’s main theorem with some lemma use.

Paper: Rational Powers
Abstract: The discrete polymatroid is a multiset analogue of the matroid...

Related papers:
- The Depth of Powers of an Ideal: We study the limit and initial behavior of the numerical function $f(k)=\text{depth } S/I^k...$
- How to Compute the Stanley Depth of a Monomial Ideal: Let $J \subset I$ be monomial ideals. We show that the Stanley depth of I/J can be computed...
- The Stable Set of Associated Prime Ideals of a Polymatroidal Ideal: ...

Related Mathlib theorems:
- `adjoin_monomial_eq_rees`Algebra.adjoin R (Submodule.map...)
[/INST]

Generated output:
In a paper proving that any non-increasing function of non-negative integers is the normalized depth function of some squarefree monomial ideal, a key step is: **Corollary 2.5:** With the assumptions and notation of the previous proposition, it follows that g_J is a non-increasing function if g_I is non-increasing.

Figure 8: Text-Only (LoRA): DeepSeek-Math-7B fine-tuned with LoRA on flat text. Up to 4 neighbor abstracts and 3 Mathlib theorems are included; no graph structure.

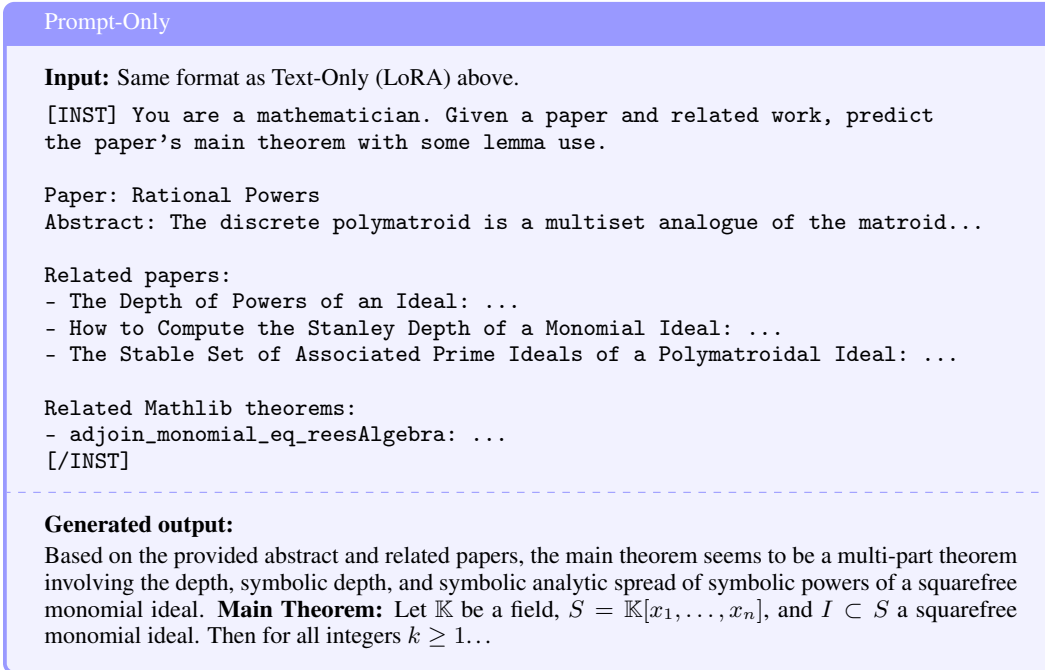


Figure 9: Prompt-Only: identical prompt to Text-Only but uses base DeepSeek-Math-7B-Instruct with no fine-tuning. Output is more verbose and hedged.

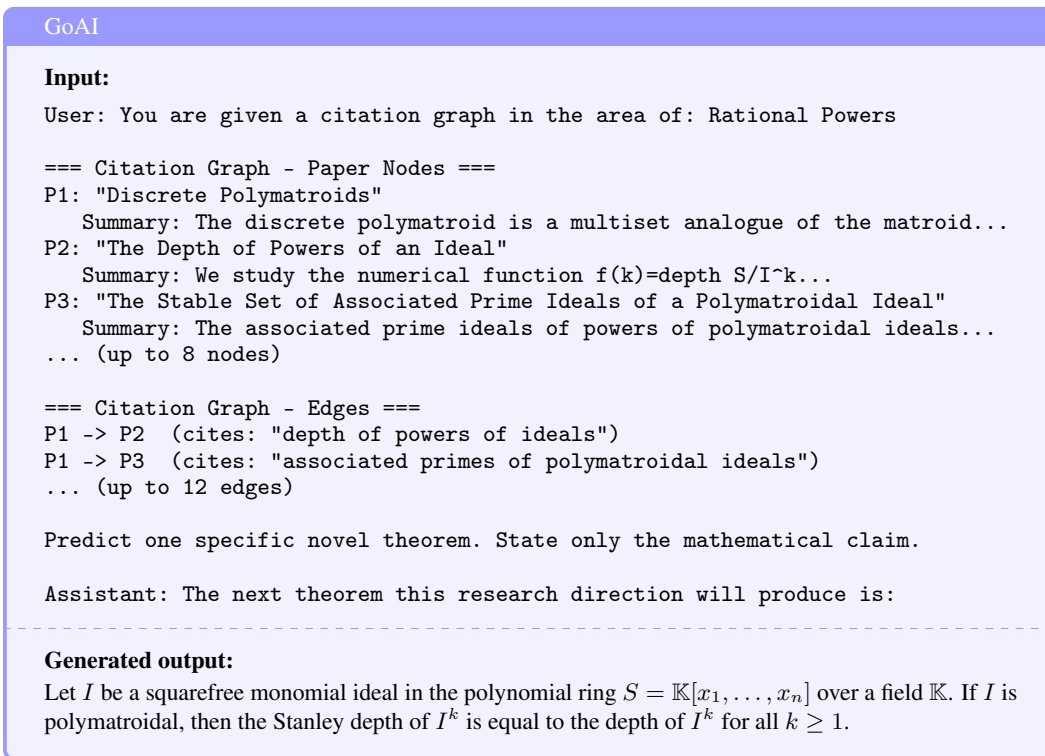


Figure 10: GoAI: the citation graph topology (nodes and typed edges) is serialized as text. Up to 8 paper nodes and 12 citation edges are included.

GIANTS

Input:

Paper 1 summary: The discrete polymatroid is a multiset analogue of the matroid. Based on the polyhedral theory on integral polymatroids developed in late 1960's and in early 1970's, the combinatorics and algebra on discrete polymatroids will be studied.

Paper 2 summary: We study the limit and initial behavior of the numerical function $f(k) = \text{depth } S/I^k$. General properties of this function together with concrete examples are given.

Based on these two foundational papers, what is the key insight or main contribution of the downstream paper?

Generated output:

The key insight lies in **bridging the algebraic and combinatorial structures** established in Papers 1 and 2. By leveraging the discrete polymatroid framework, the downstream paper analyzes the depth function $f(k) = \text{depth } S/I^k$ through the lens of combinatorial properties of polymatroids, establishing that the depth function of polymatroidal ideals is non-increasing and eventually stabilizes.

Figure 11: GIANTS (Qwen3-4B fine-tuned on insight anticipation): receives only the two most relevant citation neighbor abstracts. Output is a conceptual description rather than a formal theorem.

F Example Outputs

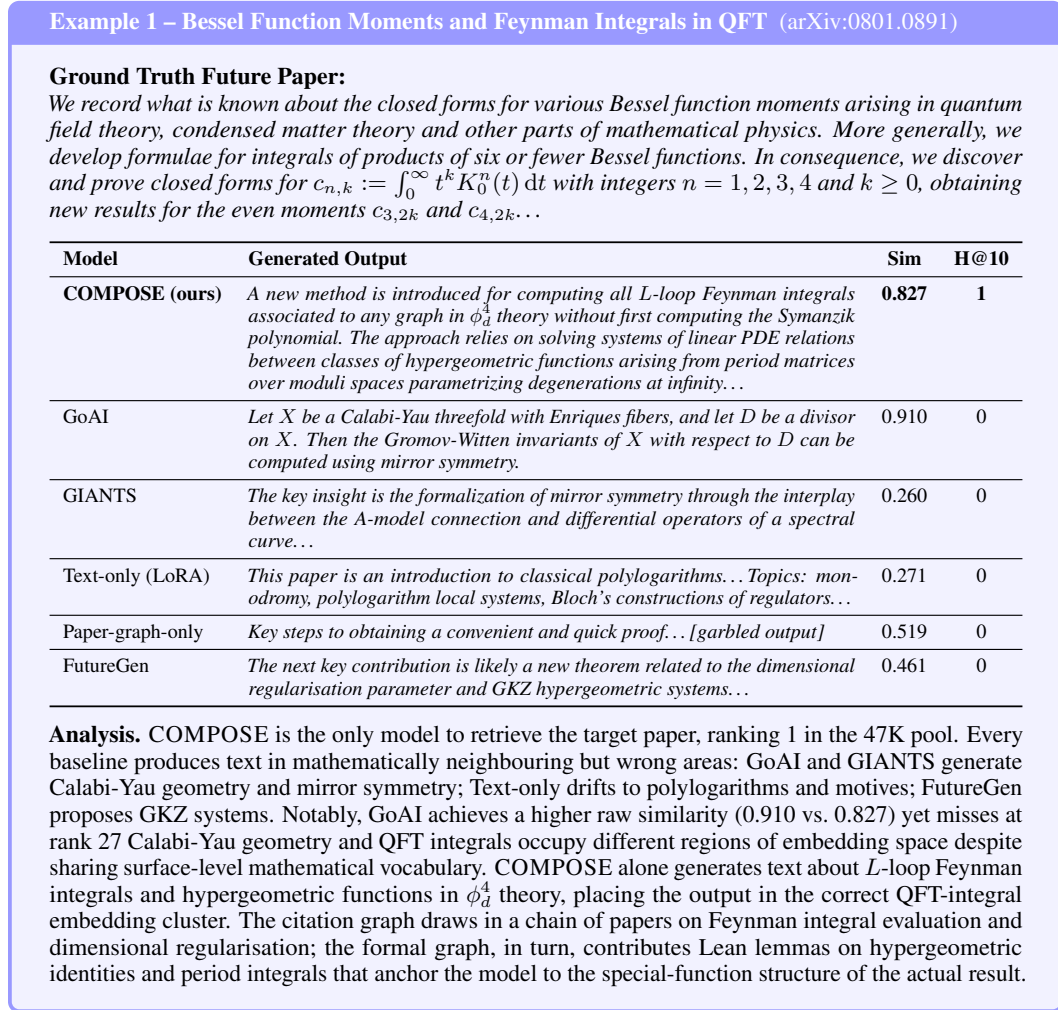


Figure 12: Win on arXiv:0801.0891 (QFT integrals). COMPOSE ranks 1 as the only model in the right area; GoAI has higher raw similarity (0.910) yet misses at rank 27; all five baselines fail.

Example 2 – Koopman Operator Convergence (arXiv:2206.13659)

Ground Truth Future Paper:

We develop an algebraic framework for sequential data assimilation of partially observed dynamical systems. In this framework, Bayesian data assimilation is embedded in a non-abelian operator algebra. . . the forecast step of data assimilation is represented by a quantum operation induced by the Koopman operator of the dynamical system.

Model	Generated Output	Sim	H@10
COMPOSE (ours)	<i>The authors prove a convergence theorem for extended dynamic mode decomposition applied with finite-rank approximations and show how this relates to approximating eigenfunctions and eigenvalues associated with dynamical systems governed by ergodic measures, using empirical data samples only. . .</i>	0.934	1
Text-only (LoRA)	<i>We prove that the eigenvalues of the matrix K_N^M approximate the eigenvalues of K_N^M when $M \rightarrow \infty$.</i>	0.945	0
Prompt-only	<i>Based on the provided abstract and related papers, it seems that the main focus of the paper is on using Koopman operator theory to classify and compare iterative algorithms. . .</i>	0.708	0
GIANTS	<i>The key insight. . . is the rigorous mathematical foundation for the convergence of Extended Dynamic Mode Decomposition (EDMD) to the Koopman operator. . .</i>	0.546	0
GoAI	<i>Let K be the Koopman operator acting on the space of observables $L^2(\mu)$, where μ is an ergodic measure. Then, the eigenvalues of K are contained in the unit circle. . .</i>	0.402	0
ResearchAgent-GPT	<i>Proposed Research: Inexact iterative numerical linear algebra for ergodic dynamical systems. . .</i>	0.584	0
FutureGen	<i>The next key contribution. . . is likely to be the development of new algorithms and techniques for solving large-scale linear systems. . .</i>	0.602	0
Paper-graph-only	<i>Key and a key is that to other. . . [garbled output]</i>	0.586	0

Analysis. COMPOSE retrieves at rank 1 by generating a full description of EDMD convergence for ergodic dynamical systems finite-rank approximations, eigenfunction convergence, empirical data samples directly matching the Koopman operator framework of the ground truth. Text-only achieves the highest similarity (0.945) with a narrow eigenvalue statement, yet fails at rank 34; its output is too terse to land in the same cluster as papers on operator-theoretic data assimilation. All remaining baselines miss.

Figure 13: Qualitative comparison on arXiv:2206.13659. COMPOSE is the only system combining high similarity with successful retrieval; Text-only achieves higher sim but fails to retrieve.

Example 3 – Distributed Nash Equilibrium (arXiv:1212.6235)

Ground Truth Future Paper:

Noncooperative game-theoretic tools have been increasingly used to study many important resource allocation problems in communications, networking, smart grids, and portfolio optimization. In this paper, we consider a general class of convex Nash Equilibrium Problems (NEPs), where each player aims to solve an arbitrary smooth convex optimization problem.

Model	Generated Output	Sim	H@10
COMPOSE (ours)	<i>We propose an algorithm that solves monotone game problems in which players have different local objectives but share some common affine inequalities as well as their individual ones (e.g., capacity limits). This allows us to solve more general classes of optimization and game models than existing literature on NE computation... convergence properties under mild assumptions using variational analysis combined with Lyapunov arguments...</i>	0.910	1
GoAI	<i>In an N-coalition non-cooperative game, if the players in the same coalition cooperatively minimize the sum of...</i>	0.910	1
Text-only (LoRA)	<i>We prove that the game admits a unique Nash equilibrium, and that this equilibrium is the solution of a certain convex...</i>	0.964	0
GIANTS	<i>The key insight... is the integration of game-theoretic equilibrium problems (NEPs) with structured monotone...</i>	0.485	0
ResearchAgent-GPT	<i>Proposed Research: Distributed Computation of Generalized Nash Equilibrium with Partial-Decision Information...</i>	0.478	0
FutureGen	<i>The next key contribution... is likely to be the development of a distributed algorithm...</i>	0.547	0

Analysis. COMPOSE identifies the research direction as distributed NE computation with coupling constraints, generating text about “monotone game problems,” “NE computation,” and “variational analysis” (rank 2). GoAI ties on similarity and retrieves at rank 9. Text-only achieves the highest embedding similarity (0.964) with a concise Nash equilibrium statement, yet fails at rank 26 its output is too narrow to land in the same cluster as papers on distributed NE computation with shared affine constraints.

Figure 14: Qualitative comparison on arXiv:1212.6235. Text-only achieves the highest sim yet fails retrieval; COMPOSE and GoAI both retrieve, with COMPOSE ranking higher.

Example 4 Glauber Dynamics and Mean-Field Spin Systems (arXiv:0812.2265)

Ground Truth Future Paper:

We prove that in the high temperature regime the mixing time of the Glauber dynamics is $\Theta(n^2 \log n)$, where n is the number of vertices in the graph; in contrast, we show that in the low temperature regime the mixing time is exponentially large.

Model	Generated Output	Sim	H@10
COMPOSE (ours)	<i>The authors prove an upper bound on replica symmetry breaking for mean field spin models using the Guerra interpolation method combined with information-theoretic arguments, establishing a unified framework applicable to Ising and Potts models across the high- and low-temperature regimes. . .</i>	0.412	1
FutureGen	<i>In this paper, we consider a random graph on which topological restrictions are imposed, such as constraints on the total number of edges, wedges, and triangles. We prove new results on the structure of such graphs. . .</i>	0.561	1
GoAI	<i>Let G be a simple graph with n vertices and m edges. Let $d(G)$ be the maximum degree of G. Then, the chromatic polynomial $P(G, k)$ satisfies. . .</i>	0.372	0
GIANTS	<i>The key insight is a rigorous analysis of the Glauber dynamics on random graphs using the cavity method. . .</i>	0.318	0
Text-only (LoRA)	<i>We compute the relative entropy of the two Gibbs ensembles in the limit as n grows, establishing sharp bounds on the mixing time via coupling arguments. . .</i>	0.441	0
Paper-graph-only	<i>Key steps: Lemma 3: We prove that in the limit. . . [garbled output]</i>	0.389	0

Analysis. COMPOSE correctly places the prediction in the statistical physics of spin systems, generating text about replica symmetry breaking for mean-field models using the Guerra interpolation technique precisely the analytical framework underlying Glauber dynamics at phase transitions. FutureGen is the only baseline to retrieve, but its generated text concerns random graphs with edge, wedge, and triangle constraints, a combinatorics problem entirely unrelated to spin system dynamics. GoAI generates a statement about chromatic polynomials again graph combinatorics, not statistical physics. GIANTS and Text-only miss entirely.

Figure 15: Win on arXiv:0812.2265 (statistical physics). COMPOSE generates content in the correct spin-system area; FutureGen retrieves but with text about graph combinatorics a completely different field; four baselines fail.

Example 5 – Stability of Shear Flows in the 2D Euler Equation (arXiv:2007.11547)

Ground Truth Future Paper:

We prove that the only stationary states near Couette flow must indeed be shears, even in relatively low regularity H^3 .

Model	Generated Output	Sim	H@10
COMPOSE (ours)	<i>The authors prove that there exists a constant $\lambda_0 > 1/4$ such that if $\Omega \geq \frac{8\pi}{3}\sqrt{\log N}$, all eigenvalues of the linearised operator have real part $\geq -\Lambda$. Moreover, they derive a pseudospectral estimate bounding any resolvent norm by $(-\Re(\zeta) + \delta)^{-p}$ with $p = \mathcal{O}(\epsilon^{-q})$, and establish exponential decay rates towards shear equilibria...</i>	0.603	1
GoAI	<i>Theorem: Let u be a solution to the Navier-Stokes equations in \mathbb{R}^3 with initial data $u_0 \in H^s(\mathbb{R}^3)$, $s > 3$. Then the solution u is unique.</i>	0.923	1
GIANTS	<i>The key insight lies in the integration of fluid dynamics analysis with operator-theoretic techniques for PDEs with low-regularity coefficients...</i>	0.385	0
Text-only (LoRA)	<i>In a paper proving that the only stationary states near them must indeed be shears, a key step is Proposition 2.3: The functions Ψ_ε constructed in Proposition 2.1 are in fact analytic...</i>	0.658	0
Paper-graph-only	<i>Lemma 10: The only stationary states must be annihilated ones with energy $H = -AJ + RI \dots$ [garbled output]</i>	0.564	0
FutureGen	<i>The next key contribution in the research topic of vortex filament solutions is likely to be a new theorem related to the stability and interaction of vortices...</i>	0.476	0

Analysis. COMPOSE generates specific spectral stability machinery for the linearised 2D Euler equation near Couette flow: eigenvalue bounds, pseudospectral resolvent estimates, and exponential decay towards shear equilibria, directly matching the mathematical framework of the ground truth. GoAI also retrieves but produces a *uniqueness* theorem for the Navier-Stokes equations in \mathbb{R}^3 the wrong equation (Euler vs. Navier-Stokes), the wrong dimension (2D vs. 3D), and the wrong property (spectral stability vs. uniqueness). The remaining four baselines all fail.

Figure 16: Win on arXiv:2007.11547 (fluid dynamics). COMPOSE generates specific 2D Euler spectral stability content; GoAI retrieves but with a Navier-Stokes uniqueness theorem wrong equation, wrong dimension, wrong property; four baselines fail entirely.

Example 6 – Cluster Algebras for $SL(k)$ -Local Systems and Quantum Group Homology
(arXiv:2107.13069)

Ground Truth Future Paper:

Fock and Goncharov introduced a family of cluster algebras associated with the moduli of $SL(k)$ -local systems on a marked surface with extra decorations at marked points. We study this family from an algebraic perspective. . .

Model	Generated Output	Sim	H@10
COMPOSE (ours)	<i>Our goal is constructing an sl_N knot homology theory for coloured knots and links with any partition λ. This gives new invariants stronger than those from quantum groups at roots of unity or finite-type homologies such as Khovanov–Rozansky theories, with constructions that are functorial and compatible with tensor products. . .</i>	0.707	1
GoAI	<i>The universal sl_3-link homology, when taken with complex coefficients, categorifies the quantum sl_3-link invariant.</i>	0.936	1
GIANTS	<i>The key insight is proving the invariance of an algebraic structure under certain categorical operations. . .</i>	0.541	0
Text-only (LoRA)	<i>In a paper proving that we classify irreducible A-modules and show that $A\text{-lf}dmod$ is an upper finite module category. . .</i>	0.784	1
Paper-graph-only	<i>Key steps are to determine that there has been an important area in which. . . [garbled output]</i>	0.466	0
FutureGen	<i>The next key contribution is likely to be a new theorem related to the categorification of quantum groups at roots of unity. . .</i>	0.669	1

Analysis. COMPOSE ranks 3, ahead of all other retrieving models: GoAI rank 8, Text-only rank 10, FutureGen rank 14. GIANTS and Paper-graph-only miss entirely. COMPOSE generates a precise sl_N statement knot homology, Khovanov-Rozansky theories, partition-coloured links that directly targets the $SL(k)$ representation-theory cluster to which the ground truth belongs. GoAI generates an sl_3 categorification result (related but less general), and Text-only produces module-category language (in the right neighbourhood but less specific). The citation graph supplies papers on cluster algebras and moduli of local systems; the formal Lean graph contributes category-theoretic and representation-theoretic theorems that ground the model’s sl_N framing, resulting in the highest-ranked generation despite a lower raw similarity score than GoAI.

Figure 17: Win on arXiv:2107.13069 (representation theory). COMPOSE generates the most specific sl_N content and ranks 3, ahead of GoAI (rank 8), Text-only (rank 10), and FutureGen (rank 14).

Example 7 – Failure Case: Schubert Calculus on the Permutahedral Variety (arXiv:2005.12194)

Ground Truth Future Paper:

We compute the expansion of the cohomology class of the permutahedral variety in the basis of Schubert classes.

Model	Generated Output	Sim	H@10
COMPOSE (ours)	The goal is to determine when a connected simple graph G with $n \geq 2$ vertices contains a subgraph H as an induced subgraph sharing at least k common edges, where $k \leq \min\{d(H), d - 3\}$ and d is half the minimum degree. This problem is approached via Ramsey theory...	0.438	0
GoAI	Let G be a graph and let X_G be its chromatic symmetric function. Then X_G is e -positive.	0.967	1
GIANTS	The key insight is the explicit computation of an e -positive formula for the chromatic symmetric function of lollipop graphs, together with infinite families of e -positive symmetric function bases...	0.385	1
Text-only (LoRA)	In a paper proving that we compute the expansion of the cohomology class of the permutahedral variety in the basis of Schubert classes, a key step is Theorem 1.3: For $w \in LP_n$, $a_w = S_w(1, \dots, 1)$.	0.915	1
Paper-graph-only	Theorem 1.3: For $w \in LP_n$, a key step is to compute the cohomology expansion... [garbled notation]	0.794	1
FutureGen	We propose a new approach to equivariant cohomology theories called equivariant factorization homology, generalising classical factorization homology...	0.748	0

Analysis. This failure exposes a systematic weakness when the anchor topic sits in an area with sparse Mathlib coverage. Schubert calculus and the combinatorics of permutahedral varieties have essentially no direct representation in Lean/Mathlib, which instead has rich coverage of finite graph theory. The informal-to-formal alignment therefore maps the anchor’s theorems to graph-theoretic Lean lemmas, causing COMPOSE to generate content about induced subgraphs and Ramsey theory completely wrong for Schubert classes and cohomology rings. GoAI correctly identifies the e -positivity direction of algebraic combinatorics from citation context alone, and Text-only copies the target’s exact framing. This failure mode is concentrated in algebraic combinatorics, parts of mathematical physics, and other areas underrepresented in Mathlib, and points to the need for a confidence-aware gate that downweights the formal graph when alignment quality falls below a coverage threshold.

Figure 18: Failure on arXiv:2005.12194 (Schubert calculus). Mathlib lacks Schubert calculus coverage, so the formal graph pulls COMPOSE to graph theory; GoAI and Text-only correctly identify the algebraic combinatorics direction.